이학박사 학위논문

A Size Effect of Nanoparticles for Arsenic Removal and Fischer-Tropsch Reaction

비소 제거 및 피셔-트롭쉬 반응에서

나노입자의 크기 효과

2014년 2월

서울대학교 대학원

협동과정 나노과학기술전공

이 승 호

A Size Effect of Nanoparticles for Arsenic Removal and Fischer-Tropsch Reaction

지도 교수 이 진 규

이 논문을 이학박사 학위논문으로 제출함
2013년 10월

서울대학교 대학원
협동과정 나노과학기술전공
이 승 호

이승호의 이학박사 학위논문을 인준함
2013년 12월

위 원 장 박 원 철 (인)

부위원장 손 병 혁 (인)

위 원 이 동 환 (인)

위 원 윤 태 종 (인)

위 원 이 진 규 (인)

Abstract

A Size Effect of Nanoparticles for Arsenic Removal and Fischer-Tropsch Reaction

Seung-Ho Lee
Interdisciplinary Program in Nano Science and Technology
The Graduate School
Seoul National University

Metal oxide nanoparticles have become an area of growing interest and importance in a wide range of fundamental studies and technological applications, due to their unique optical, electronic, magnetic, chemical, and mechanical properties. Furthermore, metal oxides nanoparticles are increasingly being associated with important environmental processes occurring in water and catalysts in synthetic fuel processes. In this thesis, we demonstrate Iron and cobalt oxide nanoparticle for environmental and catalytic application.

In Chapter 1, we briefly summarized magnetic iron oxide nanoparticle, nano for oil and gas, and Design, synthesis, and use of cobalt-based Fischer-Tropsch synthesis catalysts.

In Chapter 2, Magnetic multi-granule nanoclusters (MGNCs) were investigated as an inexpensive means to effectively remove arsenic from aqueous environment, particularly groundwater sources consumed by humans. Various size MGNCs were examined to determine both their capacity and efficiency for arsenic adsorption for different initial arsenic concentrations. The MGNCs showed highly efficient arsenic adsorption characteristics, thereby meeting the allowable safety limit of 10 μg/L (ppb), prescribed by the World Health Organization (WHO), and confirming that 0.4 g/L and 0.6 g/L of MGNCs were sufficient to remove 0.5 mg/L and 1.0 mg/L of arsenate (AsO_4^{3-}) from water, respectively. Adsorption isotherm models for the MGNCs were used to estimate the adsorption parameters. They showed similar parameters for both the Langmuir and Sips models, confirming that the adsorption process in this work was active at a region of low arsenic concentration. The actual efficiency of arsenate removal was then tested against 1 L of artificial arsenic-contaminated groundwater with an arsenic concentration of 0.6 mg/L in the presence of competing ions. In this case, only 1.0 g of 100 nm MGNCs was sufficient to reduce the arsenic concentrations to below the WHO permissible safety limit for drinking water, without adjusting the pH or temperature, which is highly advantageous for practical field applications.

In Chapter 3, Fischer-Tropsch synthesis (FTS) reaction is a reaction used for producing hydrocarbon compounds from a gas mixture (syngas) containing carbon

monoxide and hydrogen generated by reforming natural gas, gasification of coal, or biomass. This study provides a novel cobalt-based catalyst having an improved catalytic activity and stability, concurrently with an enhanced selectivity for liquid and high melting point hydrocarbons, at the expense of a low methane selectivity over conventional cobalt-based Fisher-Tropsch catalysts. We report on the conversion of synthesis gas to $C5^{+}$ with enhanced FTS activity by a factor of 5, applying catalysts that constitute cobalt nanoparticles (using a polyether and promoters) homogeneously dispersed on silica supports.

Keywords: Arsenic removal, Iron oxide, Magnetic nanoparticle, Fischer-Tropsch synthesis, cobalt oxide, Particle size effect

Student Number: 2004-30162

Contents

List of Tables

Chapter 2

Chapter 3

List of Figures

Chapter 1

Chapter 2

Chapter 3

Chapter 1

Research Background

1.1. Magnetic Iron Oxide Nanoparticles for Arsenic Removal

For the past decade, the development of methods for synthesis of superparamagnetic nanoparticles has been the center of research not just in the basic sciences but in various applied technical fields: magnetic storage media, medical applications, such as targeted drug delivery, contrast agents in magnetic resonance imaging (MRI), biosensing applications, and magnetic inks for jet printing. The properties of nanocrystals are strongly affected by the size of nanoparticles, therefore maintaining a monodisperse size is very important.[1]

Progress in the development of magnetic nanoparticle synthesis methods allowing for the adjustment of composition and size over a wide range has been remarkable over the last ten years. Various types of spherical nanocrystals the composition and particulate size of which can be adjusted are being synthesized through various chemical synthesis procedures: thermal decomposition of metal-surfactant complexes, polyol processes, sol-gel reactions, coprecipitation, reactions in constrained environments, flow injection synthesis, and aerosol methods. However, the synthesis of high-grade magnetic nanoparticles through a consistent process where an even group of magnetic particles can be formed, and a detailed understanding of the synthesis mechanisms of nucleation and growth in the process of formation of the particles, are still pending. To guarantee an economically feasible industrial mass synthesis process for iron oxide nanoparticles, which is characterized by high crystallinity, a process that

can be reproduced and does away with the need for a difficult purification process. The fundamental long-term instability associated with nanoparticles is an unavoidable problem. To reduce the energy due to the high surface area/volume ratio of nanoparticles, small particles form agglomerates. As a result, it is important to develop coating technologies to enhance the chemical stability of magnetic nanoparticles.[1]

Iron oxides exist naturally in various forms, including magnetite (Fe_3O_4), maghemite (g-Fe_2O_3) and hematite (a-Fe_2O_3), the most common. These three oxides are also technologically very important.[2] Hematite is the iron oxide discovered earliest, and is distributed widely in rocks and soil. It is also known as ferric oxide, red ochre, iron sesquioxide, specular iron ore, specularite, kidney ore, or martite. Fine hematite is red, and in the form of a rough crystal, the color is black or grey. It is very stable in atmospheric conditions, and is often the final product of the transformation of another oxide.[2] Magnetite is also known as black iron oxide, loadstone, magnetic iron ore, ferrous ferrite, or Hercules stone. It exhibits the strongest magnetism of any transition metal oxide.[2,3] Maghemite is weathering products of magnetite that are found in soil. It is metastable when compared to hematite, and form a solution with magnetite.[3,4]

Global interest in the development of waste water treatment technologies continues to grow. The utilization of iron oxide nanomaterial is the focus of

much attention, due to the very small size, surface area to volume ratio, the possibility of surface modification, outstanding magnetic properties and great biocompatibility. Many environmental purification technologies using iron oxide nanomaterial as a nanosorbent and photocatalyst in wastewater treatment. Iron oxide-based immobilization technologies for the improvement of removal efficiency are the subject of innovation research tasks.[5]

1.2. Nano Technology for Oil and Gas

Nano technology is a powerful new technology that allows for the manipulation, analysis and control of materials at the level of individual atoms and molecules, and is a foundational technology that can bring about a revolution in next-generation technologies and industry. It is expected that profound changes will be effected in social, economic, and ecological relationships.[6]

Lux Research of the United States defines nano technology as 'The purposeful engineering of matter at scales of less than 100 nanometers to archive size-dependent properties and functions.' Nano technology as defined here does not simply refer to small scales, but significant changes to properties and function at sizes less than 100 nanometers, through which some purpose must be created.[7]

Nano technology is differentiated from existing technologies and industries. First is its multi-disciplinary property, involving the parallel bridging of existing disciplines, including physics, chemistry, material sciences, electronics, and biology, and the elimination of the barriers dividing them, to create new domains and synergy effects. Second, the technology is extremely technologically intensive, as the processes of analysis, control, and synthesis of nano structures must be controlled at the nanometer level. Third, the technology is able to completely replace existing markets or create new markets, with applications in

all industrial fields including materials, electronics, optics, energy, aerospace, medicine and pharmaceuticals, therefore has extremely large economic and technological ripple effects. Fourth, as nano structures are synthesized at ultra-small scales, efficiency can be maximized through minimal consumption of raw materials, and pollution and waste can be suppressed. The technology is also characteristically environmentally friendly, with the use of clean energy through high-efficiency solar cells, for example. Fifth, the use of an understanding of the natural principles governing the structuration of atoms or molecules in nature to develop technologies for their artificial control is very eco-friendly. Technologically, nano technology is radical. Industrially speaking, it is disruptive, and socially, it is transformative. It is an enabling general purpose technology (GPT) that provides new possibilities in most industrial fields, with the potential for tech innovation in existing industries and the creation of new industries, therefore is a source of new academic disciplines and growth-driving industries.[6]

The following was published in the column “The Choice is Yours” by Gregor Wolbring, under the title “Nano for Oil and Gas.” A recent article published in the ‘Oil & Gas Journal,’ titled ‘Nanotechnology Seen Boosting Recovery Factors,’ claims that nano technology will soon boost the average production of oil and gas by up to 10%, with nano technology research in the oil and gas industries progressing at a very rapid pace. It is forecast that the use

of applied nano technologies will explode in the gas and oil fields within the coming 5 years. It is very surprising that whereas my columns cover applied nano technologies in numerous fields, there is very little in the public domain regarding nano for gas and oil. Searching the Oil and Gas Journal only turns up a few articles mentioning nano. An article published in the Oil & Gas Journal. Oct 20, 2008. Vol. 106, Iss. 39, mentions a nano-catalyst that shatters the stereotype that “oil is dirty.” It reads “it has the potential to clean the bitumen in natural underground reservoirs, and reduces the need for tailing ponds.” In Oil & Gas Journal. Oct 6, 2008. Vol. 106, Iss. 37, the article “New technologies targeting changing feeds, products challenges” mentions that “new hydroprocessing technologies using slurry nano catalysts will be applied to residual petroleum conversion, a rich future fuel source.” Oilweek mentions that nano-CT is able to visualize tight gas sands, tight shales and tight carbonates with smaller pore structures that can be detected with existing micro-CTs. Nanotechnology that allows for the extraction of more oil from wells has been developed by the research team at The University of Queensland's Australian Institute for Bioengineering and Nanotechnology (AIBN). Pepfactants® is a nano technology product that is used for emulsion and foam control in a wide variety of industrial processes including the oil industry. It is also expected that nano technology will have applications in recovery processes involving the recovery and reuse of leaked oil.

Lux Research's report ''Petroleum Players Seek Nanotech Solutions to Oil Supply Woes," discusses how nano technology could contribute to the discovery of new oil fields in the oil and gas industry, and increased production at existing wells. The report mentions that "underground oil exists in nano-sized pores. The extreme temperatures and pressures at oil wells are advantageous to nano-structure materials and coatings, and nano catalysts can upgrade crude oil to high added value products."

Given this marketability, it is not surprising that a focus has been placed on nano technology for oil and gas. Associations like the Society of Petroleum Engineers and the Advanced Energy Consortium are studying everything from surface nano sensors to autonomous nanobots. Scientists at the Argonne National Laboratory of the US Department of Energy are combining fine boric acid molecules with existing motor oils to improve lubrication properties and energy efficiency.

Aramco of Saudi Arabia has recently been investing billions in research and development, raising interest in nano technology development through SPE workshops, while AEC of the United States is developing nano technologies with research funding from ten oil and gas companies. As is evident from the subjects of the 'Nanotech' conference, discussion into nanotechnology development in the oil and gas industry is well accounted for. Recently overseas, oil and gas companies' efforts to utilize nano technologies have been picking up

speed.

Whereas Korean universities, research institutes and corporations are focusing investment into nano technologies, attempts in fields relating to the oil and gas industries are few and far in between. Domestic research is achieving substantial commercialization success in the fields of IT and bio technology (BT), however performance in the energy sector is low.

Major oil companies are at the center of efforts to apply nano technologies to the oil and gas sector. They are attempting to develop oil fields that could not be reached with existing technologies, and to improve productivity of oil wells by applying nano technologies.

The Advanced Energy Consortium (AEC)[8] is a research consortium with 30 million dollars in research funds to develop surface micro and nano sensors able to identify reservoir rock formations and component materials in 3-dimensional space. AEC recruits the best scientists and engineers from the industrial and academic fields around the world, and performs the role of center point for joint research and technological networking. Participants have the shared goal of proliferating technologies that shed new light on gas and oil reservoirs to allow for the most efficient extraction and production from reserves. It aims to supply stable and sustainable energy for the current and future generations. AEC is a leader in pre-competitive research in the micro and nano technology fields, with

a focus on sensors, devices and materials to create positive disruptive changes in enhancing the recovery rate of oil and gas from new and existing reservoirs.

Research performed in universities around the world will greatly enhance oil and gas production capabilities, especially contributing to advances in areas where the most recent production technologies have failed in increasing oil and gas recovery rates. Generation of basic research that cannot be performed without research funding support from the AEC. Some research begins at the micro level, but approaches the nano level as research progresses.

The Advanced Energy Consortium was formed by ten major energy corporations and energy service companies to improve productivity for upstream oil and gas through applied nano technologies. The Bureau of Economic Geology at the University of Texas at Austin manages the program, and, according to demands by the board of directors, Rice University leads the technical direction. As the first organization of its kind in the field of oil and gas, the organization aims to meet the requirements of all member companies, and realize the goal of increasing supply, which is a critical economic element, to satisfy both shareholders and humanity in general. The 10 participating companies are contributing $1M to the AEC budget each year. Whereas many researchers worldwide are pursuing research into alternative energies and energy storage, with the middle class populations of China and India expected to grow continuously in the coming 20 years, demand for energy to meet demand

will increase. AT the same time, we are faced with a reality of dwindling government investment into gas and oil production technologies, and a decrease in the ability to extract enough oil and gas to meet demand.

In the mid to long-term, the AEC aims to use the new properties of nano-scale materials and devices to offset this imbalance, so as to improve the productivity of member corporations. As more than 60% of reserves lie untapped due to physical or geological reasons, even a 10% increase in productivity will buy ample time to seek realistic and appropriate replacement energy supplies.

Of course, the billions of Dollars' worth of economic impact had by 10% in "additional" oil and gas cannot be dismissed. Such a change could improve the ability of western economies to cope with financial crises, and create profits for member corporations. Also, the research performed in the directions proposed by AEC will contribute to building nanoscience knowledge, creation of solutions, productivity, business opportunities, increased employments and profits in various applied fields including aerospace, pharmaceuticals and the electronics industry. Whereas previously most nano and micro research was performed outside the oil and gas industry, the AEC is performing an important role in the energy industry, focusing attention to nanoscale solutions to energy problems. AEC is operated through research funds contributed by 10 oil and gas-related companies, with the BEG responsible for general management and

operations and the Smalley Institute providing technological support. The ten participating companies are BP, BakerHughes, ConocoPhillips, Halliburton, Marathon, Occidental, Petrobras, Schlumberger, Shell, and Total.

Ten percent of the initial research tasks were in the materials field, with 90% of funding going to micro and nano sensor development. Other tasks include magnetic imaging proves, transport of fluids using carbon nano tubes, and recovery of petroleum through nano channels. Research tasks are focused in two major areas. The first area of focus is nano sensors, with research being performed under a long-term development plan. The area handles deployment and retrieval, transport, sensing, communication, power, memory, and protective devices. The second area is nano materials, a short-term program, comprising planning evaluations of feasibility and the utilization of new materials being developed in over industrial sectors.

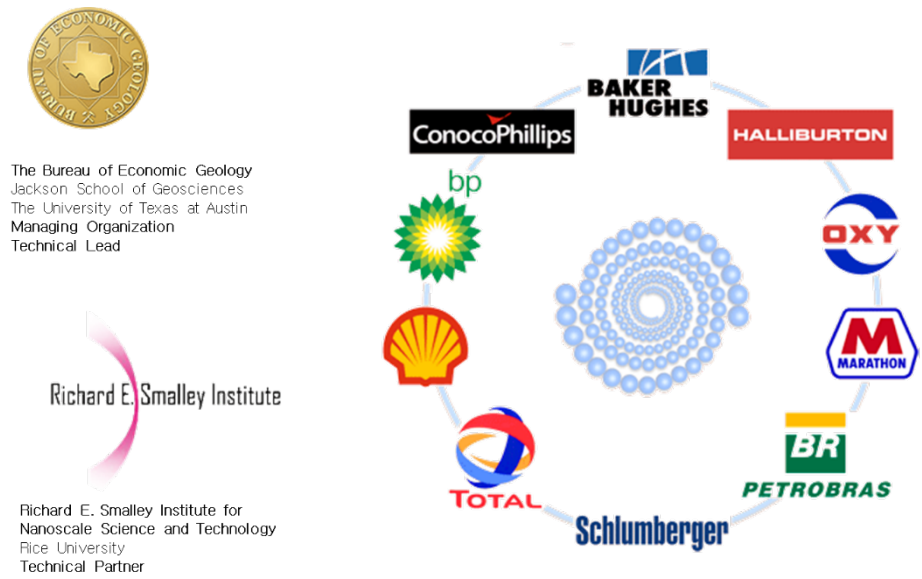

Figure 1-1. The Advanced Energy Consortium (from Ref. [8] http://www.beg.utexas.edu)

The vision of the Smalley Institute of Nanoscale Science & Technology[9] is to take the lead in resolving the problems causing the most grief to humanity through nano technologies. The institute supports and promotes research into nano technologies to tackle the challenges that face all humans around the world while providing experienced intellectual leadership, a solid management organization, scientific infrastructure of a global standard, a productive community, and relations with industries and governments. Rice University's "Richard E. Smalley Institute for Nanoscale Science and Technology" is an institution established by the university focused on promoting the enhancement of current plans in science and technology, and future success, at the nanometer level. The research institute provides active support for Rice University's nanoscience and technological interests. In 2002 and 2003, Professor Richard E. Smalley developed a list of 10 challenges to humanity in the 50 years to come. The Smalley Institute has taken on 5 of these challenges as research tasks: energy, water, environment, disease, and education. The faculty of the Smalley Institute has utilized various nano-technologies that profoundly impact the 5 major research challenges.

Figure 1-2. Nanotechnology at Rice (from Ref. [9] http://cnst.rice.edu)

1.3. Cobalt-based Fischer-Tropsch synthesis catalysts

With the increasing demand for clean fuel, objectives are changing in the petroleum industry. In this new situation, catalysts perform an important role. A review of the fuels with the highest potential shows that natural gas is the most attractive. Through a simple process, natural gas becomes a sulfur-free product. In the long-term perspective, it can be forecast that reliance on natural gas will increase in the refining industry, currently centered on petroleum. With rising concern over the safety issues of nuclear power, the role of natural gas is ever increasing. As the key component of natural gas is methane, an inert molecule, it is expected that interest in so-called C1 chemistry, traditionally performed through a catalyst process, will grow. When natural gas is the main raw material, there are two types of catalyst that are of interest. First is the conversion of natural gas or feedstock, the main component of which is methane, into syngas, a compound of hydrogen and carbon monoxide. Production of this syngas is performed through Fischer-Tropsch synthesis, producing a hydrocarbon in the form of synthetic crude oil known as “traditional GTL,” and conversion into other gases including dimethyl ether (DME).[10]

All group VIII metals are showing obvious activity in the hydrogenation of carbon monoxide to hydrocarbons.

$$nCO + 2nH_2 \rightarrow C_nH_{2n} + nH_2O$$

$$nCO + (2n + 1)\ H_2 \rightarrow C_nH_{2n+2} + nH_2O$$

Iron, nickel, and cobalt are the most active metals for the hydrogenation of carbon monoxide except for ruthenium. FT process is producing hydrocarbons and its average molecular weight is reduced in the following order: Ru > Fe > Co > Rh > Ni > Ir > Pt > Pd. Therefore, for commercial production considerations, only ruthenium, iron, cobalt, and nickel have catalytic characteristics. Nickel catalysts cause too much methane in practical conditions. Ruthenium is too high-priced, and global reserves are not enough for use in large factories. Cobalt and iron are the metals proposed as catalysts for syngas conversion by Fischer-Tropsch. Cobalt and iron are both used in the hydrocarbon synthesis industry. Cobalt catalyst is pricier, but has a greater deactivation resistance. The activation of the two metals is similar at low conversion rates, but cobalt catalysts have a greater productivity at high conversion rates. The water generated in FT synthesis slows reaction speed more so for iron than for cobalt catalysts. The water-gas shift reaction is more important on iron than cobalt catalysts.[11]

$$CO + H_2O \rightarrow CO_2 + H_2$$

Iron catalysts generally produce more olefins. Iron and cobalt catalyst are

both sensitive to deactivating sulfur. In the case of iron-based catalysts, syngas must not have a sulfur content of 0.2 ppm or higher. In the case of Co catalysts, the amount of sulfur contained in the raw material must be 0.1 ppm or less. Normally, cobalt catalyst on an oxide support has greater resistance to damage than iron. Therefore, cobalt catalyst is more appropriate for slurry-type reactors. Iron catalysts create hydrocarbons oxygenated compounds at various temperatures, pressures, and syngas ratios. Cobalt catalyst work in a very narrow range of temperatures and pressures, and a rise in temperature results in increased methane selectivity. As iron catalyst can be used at low H_2/CO ratios, it is more appropriate for the conversion of syngas from biomass into hydrocarbons.[11]

FT processes currently have two modes of operation, high and low temperature. In the high-temperature FT (573-623 K, HTFT) process, syngas is reacted in a fluidized bed reactor with an iron-based catalyst to create hydrocarbons within the C1-C15 range. This process is mainly used to produce liquid fuel, although many useful chemicals can be extracted from the synthetic oil. Oxygenates in the aqueous stream are isolated and purified in order to produce alcohols, acetic acid, and ketones. Both iron and cobalt catalysts can be used in low-temperature FT (473-513 K, LTFT) processes that synthesize waxes and paraffins, which are long linear chains of hydrocarbons. High-quality, low-sulfur diesel fuel is produced in this process. Most FT technology of the

last two decades is based on the LTFT process. Due to the safety of the process, high conversion rate and high hydrocarbon production rate of cobalt catalysts, they are considered the optimal choice for LTFT processes to synthesize long chain hydrocarbons.[11]

High Fischer-Tropsch synthetic catalyst, with high productivity, can reduce reactor volume and improve process economy. Normally, volumetric productivity can be adjusted by changing the density of the active sites or the characteristics of turnover rates. Supported Co catalyst with a high specific rate, therefore requires the use of a support or alloy elements that increase the rate per Co atom and small metal crystal synthesis at high surface density on the support surface. Under reaction conditions that favor the formation of short paraffin, activation of cobalt atoms on the surface of small crystals for CO hydrogenation reactions is lower than on the surface of large crystals.[12] The effect of this crystal size and support manifests in a distribution of crystal size that is not overly sensitive to crystal size,[13] and also applies where the number of Co atoms in contact with the support is a very small proportion of the total number of metal atoms that exist in the crystal. Later research shows that this observed effect of crystal size is indirect. This indicates reoxidation of the Co metal due to the water generated in the FTS reactions, or the incomplete deoxidation of the CoO. Both rely on the size of the Co crystal.[14]

The catalyst activation and selectivity of supported cobalt in FT reactions

is well known. However, because commercial FT catalyst has cobalt particle sizes of around 20nm, there is room for improvement.[15] A reasonable strategy for research to develop catalysts with better activation is to decrease the average particle size to increase cobalt dispersion. Leaders in this field, Bartholomew and Yermakov reported in 1985 that activation is greatly increased when cobalt particle size is reduced from 200 to 9nm, a result that was later repeated by Iglesia et al.[14,16] It was shown that surface-specific activity, commonly referred to as turnover frequency (TOF), is not influenced as such by cobalt particle size. However, despite further reductions in cobalt particle size, results reported in literature are fewer and father in between. Many research groups reported that for catalysts with cobalt particle size less than 10nm, TOF was drastically reduced.[17-20]

As the metal Co is the active site in FTS, efforts were concentrated on developing a new catalyst with improved metal dispersion as a reasonable strategy to increase the number of exposed cobalt atoms. From this perspective, manufacture methods such as homogeneous deposition–precipitation,[21] mixed sol–gel procedures,[22] or electrostatic adsorption of Co complexes[23] are being applied to the manufacture of Co-based catalysts with improved metal dispersion. Catalysts supports with advanced structures like mesoporous silicas,[24] high surface area carbon,[25] delaminated zeolites[26] or nanofibrous inorganic materials[27] and optimization of heat treatment in the process of

activating the precursor materials[28] are being used in manufacturing FTS catalysts consisting of very small cobalt nano particles. Still, contrary to expectations for improved catalyst activation in well-dispersed Co catalysts, reduced selectivity for long chain hydrocarbons and slow reaction speed was found.[24] The traditional explanation for reduced catalyst activation and selectivity for high molecular weight products has been the residual Co that remains oxidized after deoxidation preprocessing. This is because of the very low reductive properties owing to very small Co nanoparticles when supported using a normal inorganic support.[29]

Interest in the effect of particle size in nano catalysts is growing. Many examples are known regarding supported and unsupported particles, and it has been proven that catalyst performance relies on particle size and shape.[30,31] Much research has been performed to understand the basic nature of this effect, and this understanding is being promoted by well-structured manufacturing methods, studies into support materials and surface science research.[32]

1.4. Scope of Dissertation

There is an urgent need to improve the prevailing water treatment technology because arsenite (AsO_2^-) and arsenate (AsO_4^{3-}) are the two predominant arsenic species found in groundwater. Various types of iron-based nanoparticle adsorbents have been developed for arsenic removal because of their high affinity for and adsorption capacity of the anionic form of arsenic oxyacids. Many methods have been developed to increase the size of magnetite nanoparticles, which would result in a fast response to the external magnetic field particles, while keeping them stably dispersed in solution. To this end, it is sometimes misunderstood that large-sized superpara-magnetic nanoparticles having negligible remanence (residual magnetism) and coercivity (the field required to reduce magnetization to zero) at room temperature is the most effective material. In the present research, MGNCs were prepared in a large scale, as reported in our previous work, and examined for their capacity to remove the AsO_4^{3-} anion from water.

GTL has some advantages in actual market environment where oil price is high, but gas price is low. The development and production of rich shale gas leads to excessive supply of gas and then the gas price is formed as lower, and that constant demand of oil from China and India tend to raise oil price. The gap

between oil and gas price is anticipated to be continuously deepened. Fischer-Tropsch synthesis (FTS) reaction is a reaction used for producing hydrocarbon mixtures from a synthesis gas (syngas) containing carbon monoxide and hydrogen produced by reforming natural gas, gasification of coal, or biomass. The present study presents a novel cobalt-based catalyst having an advanced catalytic activity and stability, together with an enhanced selectivity for liquid and high melting point hydrocarbons, at the expense of a low methane selectivity over conventional cobalt-based Fischer-Tropsch catalysts.

1.5. References

(1) Laurent, S.; Forge, D.; Port, M.; Roch, A.; Robic, C.; Vander Elst, L.; Muller, R. N. *Chem. Rev.* **2008**, *108*, 2064.

(2) Cornell, R. M.; Schwertmann, U. *The Iron Oxides: Structure, Properties, Reactions, Occurrences and Uses*; Wiley, 2003.

(3) Majewski, P.; Thierry, B. *Crit. Rev. Solid State Mater. Sci.* **2007**, *32*, 203.

(4) Teja, A. S.; Koh, P.-Y. *Prog. Cryst. Growth Charact. Mater.* **2009**, *55*, 22.

(5) Xu, P.; Zeng, G. M.; Huang, D. L.; Feng, C. L.; Hu, S.; Zhao, M. H.; Lai, C.; Wei, Z.; Huang, C.; Xie, G. X.; Liu, Z. F. *Sci. Total Environ.* **2012**, *424*, 1.

(6) KISTI *Industrialization Perspective of Major Nanotechnologies*; Korea Institute of Science and Technology Information: Seoul, 2008.

(7) Lux, R. *The nanotech report*; 5 ed.; Lux Research Inc.: New York, 2007.

(8) *http://www.beg.utexas.edu*.

(9) *http://cnst.rice.edu*.

(10) Sousa-Aguiar, E. F.; Noronha, F. B.; Faro, J. A. *Catalysis Science & Technology* **2011**, *1*, 698.

(11) Khodakov, A. Y.; Chu, W.; Fongarland, P. *Chem. Rev.* **2007**, *107*, 1692.

(12) Johnson, B. G.; Bartholomew, C. H.; Goodman, D. W. *J. Catal.* **1991**, *128*, 231.

(13) van Hardeveld, R.; Hartog, F. 1972; Vol. 22, p 75.

(14) Iglesia, E. *Applied Catalysis A: General* **1997**, *161*, 59.

(15) Oukaci, R.; Singleton, A. H.; Goodwin Jr, J. G. *Applied Catalysis A: General* **1999**, *186*, 129.

(16) Iglesia, E.; Soled, S. L.; Fiato, R. A. *J. Catal.* **1992**, *137*, 212.

(17) Bezemer, G. L.; van Laak, A.; van Dillen, A. J.; de Jong, K. P. In *Stud. Surf. Sci. Catal.*; Xinhe, B., Yide, X., Eds.; Elsevier: 2004; Vol. Volume 147, p 259.

(18) Martínez, A. n.; López, C.; Márquez, F.; Díaz, I. *J. Catal.* **2003**, *220*, 486.

(19) Ho, S. W.; Houalla, M.; Hercules, D. M. *The Journal of Physical Chemistry* **1990**, *94*, 6396.

(20) Bezemer, G. L.; Bitter, J. H.; Kuipers, H. P. C. E.; Oosterbeek, H.; Holewijn, J. E.; Xu, X.; Kapteijn, F.; van Dillen, A. J.; de Jong, K. P. *J. Am. Chem. Soc.* **2006**, *128*, 3956.

(21) Bezemer, G. L.; Radstake, P. B.; Koot, V.; Van Dillen, A. J.; Geus, J. W.; De Jong, K. P. *J. Catal.* **2006**, *237*, 291.

(22) Okabe, K.; Li, X.; Wei, M.; Arakawa, H. *Catal. Today* **2004**, *89*, 431.

(23) D'Souza, L.; Regalbuto, J. R.; Miller, J. T. *J. Catal.* **2008**, *254*, 157.

(24) Panpranot, J.; Goodwin Jr, J. G.; Sayari, A. *Catal. Today* **2002**, *77*, 269.

(25) D'Souza, L.; Jiao, L.; Regalbuto, J. R.; Miller, J. T.; Kropf, A. J. *J. Catal.* **2007**, *248*, 165.

(26) Concepción, P.; López, C.; Martínez, A.; Puntes, V. F. *J. Catal.* **2004**, *228*, 321.

(27) Martínez, A.; Prieto, G.; Rollán, J. *J. Catal.* **2009**, *263*, 292.

(28) Sietsma, J. R. A.; Meeldijk, J. D.; Den Breejen, J. P.; Versluijs-Helder, M.; Van Dillen, A. J.; De Jongh, P. E.; De Jong, K. P. *Angewandte Chemie - International Edition* **2007**, *46*, 4547.

(29) Prieto, G.; Martínez, A.; Concepción, P.; Moreno-Tost, R. *J. Catal.* **2009**, *266*, 129.

(30) Van Santen, R. A. *Acc. Chem. Res.* **2008**, *42*, 57.

(31) Somorjai, G.; Tao, F.; Park, J. *Top. Catal.* **2008**, *47*, 1.

(32) den Breejen, J. P.; Radstake, P. B.; Bezemer, G. L.; Bitter, J. H.; Frøseth,

V.; Holmen, A.; Jong, K. P. d. *J. Am. Chem. Soc.* **2009**, *131*, 7197.

Chapter 2

Efficient Removal of Arsenic Using Magnetic Multi-Granule Nanoclusters

2.1. Introduction

Arsenic is highly toxic element known for its deleterious influences on both the environment and human health. High levels of arsenic uptake by humans have led to health problems such as skin-, kidney-, lung-, liver cancer, and neurological damage in the USA, China, Chile, Bangladesh, Taiwan, Mexico, Argentina, Poland, Canada, Hungary, Japan, Nepal, Vietnam, and India. The largest at-risk population to groundwater arsenic pollution is in Bangladesh, followed by the inhabitants of West Bengal in India.[1-3] Because of its toxicity and carcinogenic effects on human health, the World Health Organization (WHO) reduced the allowable safety limit of arsenic in drinking water from 50 to 10 μg/L in 1993, and strictly regulated the quality of water.[4] The European Union has amended all drinking water supply systems according to this updated limit. The United States Environmental Protection Agency (USEPA) has also adopted the WHO prescribed maximum level of arsenic contamination (10 μg/L) in drinking water; this has been put to effect since 2006.[5]

There is an urgent need to improve the prevailing water treatment technology because arsenite (AsO_2^-) and arsenate (AsO_4^{3-}) are the two predominant arsenic species found in groundwater.[6] Adsorption has become an attractive and promising technology for arsenic extraction because of its simplicity, safety, ease of operation, maintenance, and handling, sludge-free operation, potential for regeneration, and possibility for the use of inexpensive

adsorbent. In general, it is open considered to be the most effective treatment process for the removal of arsenic from aqueous environments at relatively low costs. Furthermore, to be effective and practical, an arsenic removal method should be easily applicable at individual sites serving households or small communities.[7] Various types of iron-based nanoparticle adsorbents have been developed for arsenic removal because of their high affinity for and adsorption capacity of the anionic form of arsenic oxyacids. Some of the representative examples of these types of compounds are Fe_3O_4@NiO hierarchical nanostructures,[8] ordered meso-porous carbon encapsulating a wide range of metal oxide nanoparticles,[9] Fe_3O_4 and Fe_2O_3 obtained through a precipitation method,[10] and mechanically ball-milled Fe_3O_4 nanopowder.[11]

Various studies have described the adsorption mechanism as the formation of inner-sphere complexes via ligand exchange with OH^- or OH_2 groups on ferric hydroxide.[12] Researchers have used X-ray absorption fine structure (EXAFS) spectroscopy to deduce the local coordination environment of arsenate on the mineral goethite (R-FeOOH).[13,14] Fendorf et al.[15] have reported that three distinct surface complexes exist on goethite by the arsenate-Fe distances: A monodentate complex, a bidentate-binuclear complex, and a bidentate-mononuclear complex. The kind of complex was found to be reliant on the coverage. At low surface coverage, the monodentate complex was preferred but at higher coverage the bidentate complexes were more prevalent

than the bidentate. Binuclear complex seems to be in the largest proportion at highest surface coverage.

M. Gallegos-Garcia et al.[16] explained the mechanism of arsenic adsorption on iron oxide. They emphasized that arsenic species adsorbption on iron oxide minerals in water is principally ascribed to chemical adsorption through the forming of binuclear bridging complexes Fe–O–AsO(OH)–O–Fe on the minerals, as well as electrostatic attraction and surface complexion between species and iron hydroxides on the minerals.

Many methods have been developed to increase the size of magnetite nanoparticles, which would result in a fast response to the external magnetic field particles, while keeping them stably dispersed in solution. To this end, it is sometimes misunderstood that large-sized superpara-magnetic nanoparticles having negligible remanence (residual magnetism) and coercivity (the field required to reduce magnetization to zero) at room temperature is the most effective material. However, this is not the most effective way. We recently reported that ferromagnetic materials could be made more useful when they could be dispersed in the solution by a strong interaction between solvent molecules and surface functional groups.[17] The magnetic saturation (M_S) values measured at 70 kOe (300 K) were 73.9, 80.3, and 84.6 emu/g for MGNCs of 100, 200, and 400 nm, respectively. The relatively high M_S value of multi-granule nanocluster (MGNC) samples at 100 nm was very close to the reported

M_S values for Fe_3O_4 nanoparticles. The zero-field cooling/field cooling (ZFC/FC) measurements clearly showed the ferromagnetic behavior of MGNCs with various diameters. Although the MGNCs used in our experiments are ferromagnetic are very stable in aqueous solution and are homogeneously dispersed because of multi-granule structure resulting an increased numbers of the surface functional groups (–OH). Therefore, it is of interest to use this new type of magnetite in MGNC for arsenic removal application.

In the present research, MGNCs were prepared in a large scale, as reported in our previous work,[17] and examined for their capacity to remove the AsO_4^{3-} anion from water. We find out that contaminated water could be easily remediated with magnetic MGNCs, which could effectively and practically be applied at individual sites serving households or small communities.

2.2. Experimental Section

Materials. Iron(III) chloride hexahydrate ($FeCl_3 \cdot 6H_2O$, > 97%, Sigma-Aldrich), sodium arsenate dibasic heptahydrate ($Na_2HAsO_4 \cdot 7H_2O$, > 98%, Sigma-Aldrich), sodium acetate anhydrous (NaO_2CCH_3, > 98.5%, Samchun Chemicals), and ethylene glycol ($HOCH_2CH_2OH$, > 99.5%, Samchun Chemicals) were purchased and utilized as received. An arsenic stock solution of 100 mg/L was prepared by dissolving appropriate amount of sodium arsenate $Na_2HAsO_4 \cdot 7H_2O$ in deionized water. Working solutions for each experiment were freshly prepared from the stock solution.

Preparation of MGNCs. MGNCs were prepared by following the procedure published in the literature.[17]

In a typical MGNC synthesis, $FeCl_3 \cdot 6H_2O$ (27 g, 0.1 mol), NaO_2CCH_3 (100 g, 1.2 mol) and distilled water (100 g, 5.6 mol) were completely dissolved in ethylene glycol (1.5 L) by vigorous mechanical stirring to form a yellowish-brown turbid solution. After heating the solution at 70 °C for various lengths of time, the reaction temperature was increased to the refluxing temperature to complete the reaction, leading to the formation of MGNCs. At this point, the reaction solution turned reddish-brown and then slowly became black. After being cooled down to room temperature, the black sediment was separated magnetically by attaching a strong permanent magnet to the outside of the reaction flask and then washed with ethanol and distilled water several times to

eliminate any organic and inorganic byproducts. The specific surface area of magnetic MGNCs was characterized using the Brunauer–Emmett–Teller (BET) method by measuring the nitrogen adsorption/desorption surface area (TriStar II 3020, Micromeritics, USA operated at 77 K).

Adsorption experiments and analysis. MGNCs having sizes of 100, 200, and 400 nm were used for arsenic removal. Adsorption studies were conducted with aqueous solutions having arsenic concentrations of 0.5 and 1.0 mg/L, which corresponds to the range of arsenic concentrations in contaminated groundwater. The amounts of the MGNCs used were 0.2, 0.4, 0.6, 0.8, and 1.0 g/L for each size. The solutions of arsenic mixed with MGNCs were shaken in an orbital shaker at 200 rpm, at 298 K for 24 h; the solutions occupied a total volume of 20 mL within the 30 mL glass vial. The MGNCs in the mixture were removed by magnetic decantation with a permanent magnet and the remaining water was evaluated to determine the adsorption capacity. The arsenic concentrations before and after the adsorption experiments were analyzed by means of an inductively coupled plasma-atomic emission spectrometer (ICP-AES, Shimadzu ICPS-7510).

2.3. Results and Discussion

Characterization of MGNCs. The MGNCs were prepared as previously reported by the simple reaction of $FeCl_3$ and sodium acetate in ethylene glycol, which served as both the solvent and reductant. Simple refluxing in glassware at atmospheric pressure allowed us to easily monitor changes in the color of the reaction mixtures and control the sizes of the MGNCs. The sizes of the MGNC were selected to be 100, 200, and 400 nm for experiments, as shown in Figure 2-1, because MGNCs with these features exhibited a fast response to the applied external magnetic field after arsenic removal from the aqueous solutions.

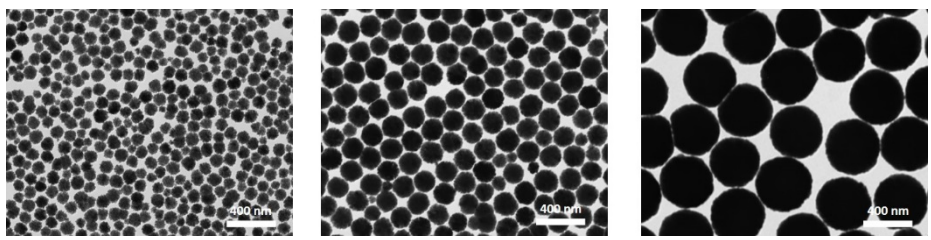

Figure 2-1. TEM images of MGNCs prepared from the molar ratios of $FeCl_3$:NaOAc:H_2O = 0.1:1.2:5.6 in 1.5 L of ethylene glycol after heating at 70 °C for (a) 1 h, (b) 12 h, and (c) 35 h. (scale bar: 400 nm)

Table 2-1. BET surface areas of various size MGNCs and commercial iron oxide (< 5 μm)

MGNC Size (nm)	100	200	400	< 5 μm Bulk Fe_3O_4
Surface Area (m^2/g)	29	14	9.3	5.1

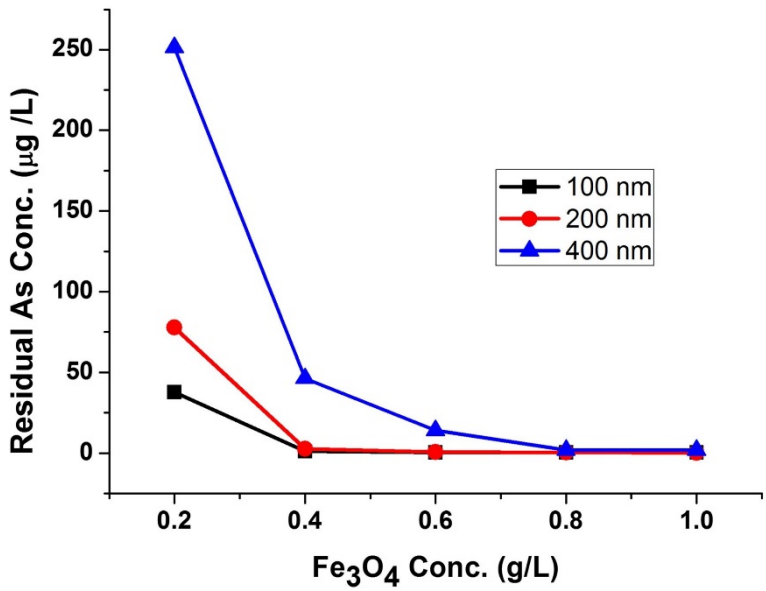

Figure 2-2. As(V) adsorption on magnetic MGNCs of different sizes (100, 200, and 400 nm); Initial arsenic concentration is 0.5 mg/L.

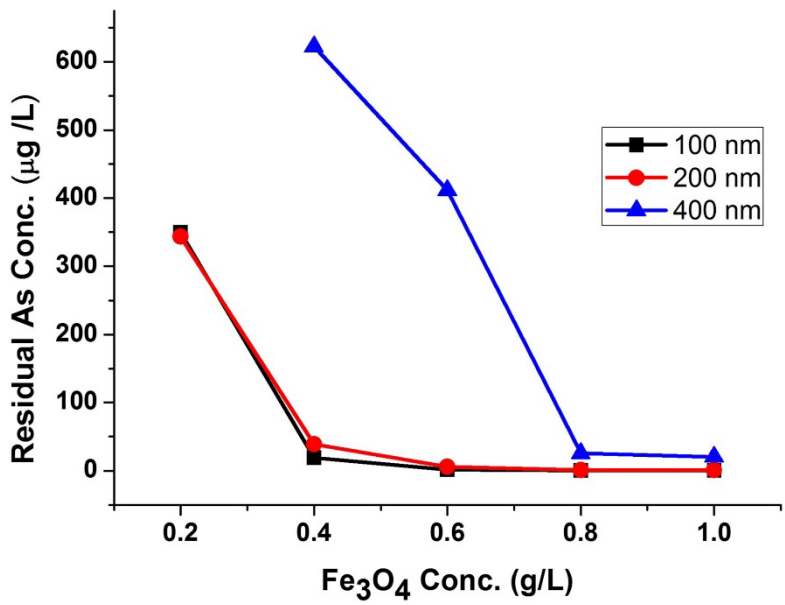

Figure 2-3. As(V) adsorption on magnetic MGNCs of different sizes (100, 200, and 400 nm); Initial arsenic concentration is 1.0 mg/L.

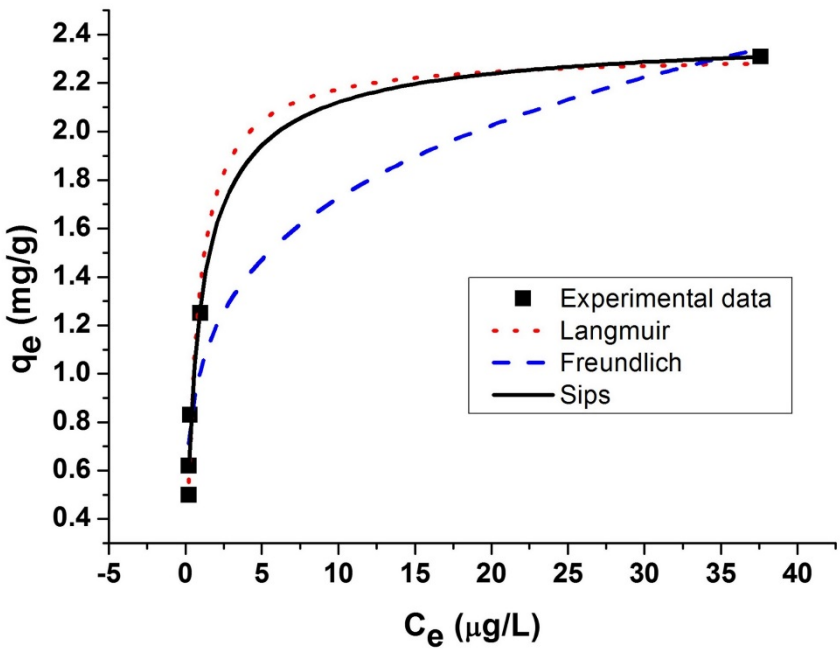

Figure 2-4. Isotherm plots based on three models for arsenic adsorption on MGNCs of different sizes; 100 nm.

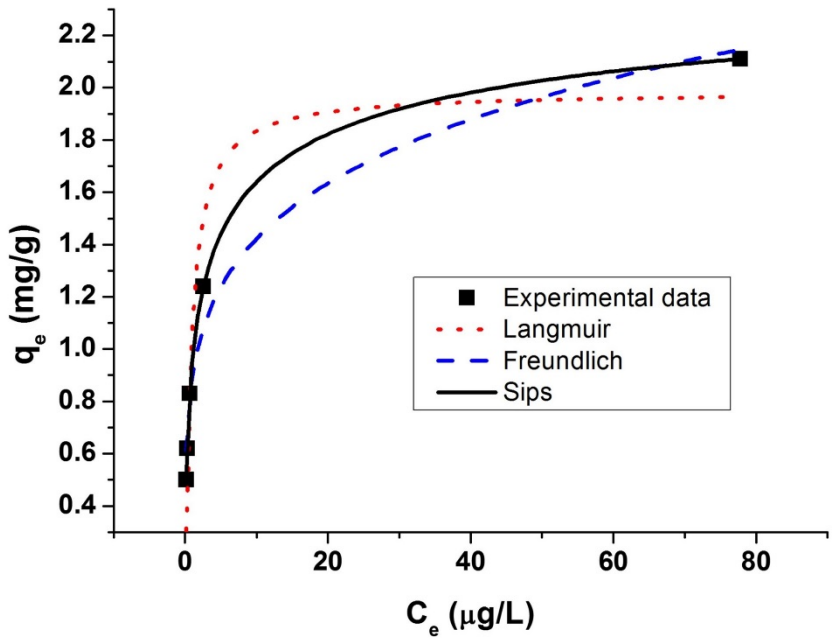

Figure 2-5. Isotherm plots based on three models for arsenic adsorption on MGNCs of different sizes; 200 nm

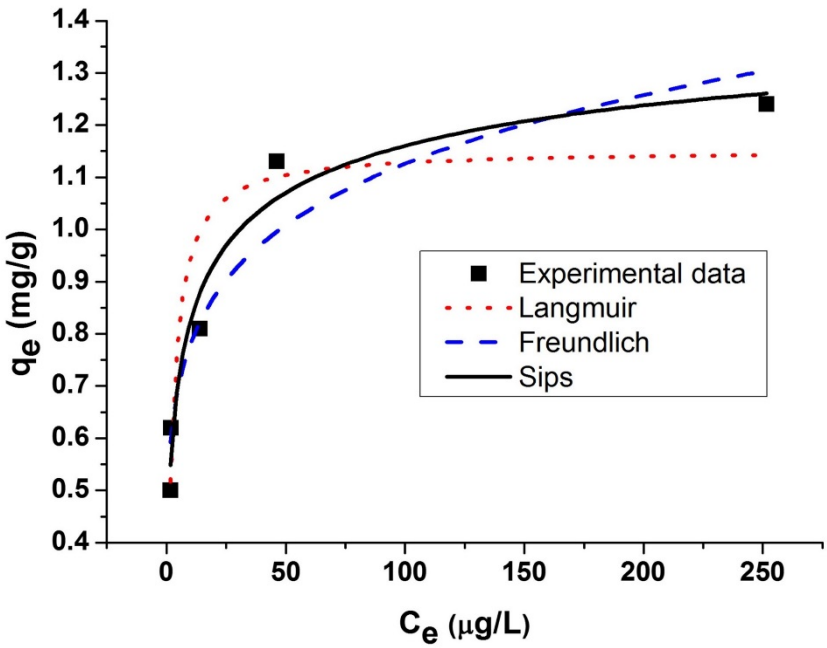

Figure 2-6. Isotherm plots based on three models for arsenic adsorption on MGNCs of different sizes; 400 nm

The specific surface area of the MGNCs was estimated using the BET method as shown in Table 2-1. As expected the surface area decreased significantly as the size of MGNC was increased; the surface area for the 400 nm size MGNC was still larger (about 2 times) than that of the bulk (< 5 μm) magnetite powder, confirming the characteristic multi-granular shape of MGNC.

Effect of initial arsenic concentration and amount of MGNCs of each size. The maximum capacity of adsorption can be increased when the initial arsenic concentration is relatively high with respect to the values found in groundwater; however, we measured adsorption capacity at arsenic concentration of 0.5 and 1.0 mg/L because these values are more representative of contaminated groundwater. As shown in Figure 2-2, when the initial concentration of As(V) was 0.5 mg/L, 100 nm MGNC could remove more than 90% of the arsenic at a concentration of 0.2 g/L. At the same initial arsenic concentration and the same size of MGNC, 0.4 g/L of the MGNC (residual arsenic was actually measured as 1 μg/L) was efficient to remove arsenic to satisfy the WHO's allowable limit of 10 μg/L. When 200 nm MGNC was used, although the adsorption efficiency appeared to be slightly decreased, the WHO's allowable limit could still be achieved at conditions of 0.4 g/L (residual arsenic was actually measured as 3 μg/L). The largest size MGNC (400 nm), used in the adsorption experiments, showed the lowest arsenic removal efficiency, as expected. At this size, 0.8 g/L MGNC was needed to satisfy the WHO limit.

These trends can be explained by the differences in the surface areas of MGNCs as shown in Table 2-1.

When the initial concentration of As(V) was increased to 1.0 mg/L, a larger amount of MGNCs was needed to remove the arsenic, and the residual arsenic concentrations were measured as 1.5 and 6 μg/L at the conditions of 0.6 g/L of 100 and 200 nm MGNCs, respectively (Fig. 2(b)). However, for 400 nm MGNC, the WHO's limit could not be achieved even at 1.0 mg/L of the MGNC.

Adsorption isotherm. Data for the equilibrium arsenate adsorption onto various size MGNCs, as shown in Figure 2-2 and 2-3, were fitted against the two-parameter Langmuir and Freundlich isotherm models and the three-parameter Sips isotherm model, as shown in Figures 2-4 ~ 2-6. The Langmuir isotherm model assumes that the adsorption occurs at specific homogeneous sites within the adsorbent. This means that once an adsorbate molecule adheres to a site, no additional adsorption can occur at that site.[18] We can assume that at low adsorbate concentrations, it effectively reduces to a linear isotherm, and thus obeys Henry's law. Alternatively, at high adsorbate concentrations, it leads to a constant monolayer sorption capacity.[19] The Freundlich isotherm model can be applied to nonideal sorption on heterogeneous surfaces, as well as multilayer sorption. Frequently, the fundamental thermodynamic basis is required because the Freundlich isotherm model does not reduce to Henry's law at low concentrations.[19] The Sips model, also known as the combined Langmuir-

Freundlich isotherm, is a three-parameter isotherm model developed to enhance the performance of the individual two-parameter models.[20] The Langmuir-Freundlich name originates from the restraining performance of the equation and the resulting model has characteristics of both the contributing models. At low adsorbate concentrations, it effectively reduces to the Freundlich isotherm, and thus does not obey Henry's law. At high adsorbate concentrations, it predicts the monolayer sorption capacity aspect of the Langmuir isotherm.[19]

The mathematical descriptions for the isotherm models are shown as follows: Langmuir (Equation 1), Freundlich (Equation 2), and Sips (Equation 3)

$$q_e = (b \cdot Q_o \cdot C_e)/(1 + b \cdot C_e) \quad (1)$$

$$q_e = K_F \,.\, C_e^{1/n} \quad (2)$$

$$q_e = [Q_s \cdot (a_s \cdot C_e)^s] / [1 + (a_s \cdot C_e)^s] \quad (3)$$

q_e is the equilibrium adsorption capacity ($mg \cdot g^{-1}$);

b is theLangmuir constant related to adsorption intensity ($L \cdot mg^{-1}$);

Q_o is the Langmuir constant reflecting the theoretical maximum adsorption capacity;

C_e is the equilibrium arsenic concentration after adsorption process ($mg \cdot L^{-1}$);

K_F is the Freundlich constant related to adsorption capacity; n is the Freundlich isotherm exponent;

Q_s is the saturated Sips model adsorption capacity;

a_s is the Sips isotherm constant; and

s is the Sips isotherm exponent.

Table 2-2. Isotherm equation parameters for arsenic removal by GNCs

Parameters	Size of Adsorbents		
	100 nm	200 nm	400 nm
Langmuir			
Q_o ($mg \cdot g^{-1}$)	2.322	1.985	1.153
b ($L \cdot mg^{-1}$)	1.471	1.223	0.455
R^2	0.978	0.877	0.821
Freundlich			
K_F ($mg \cdot g^{-1}$)($L \cdot mg^{-1}$)$^{1/n}$	1.016	0.897	0.540
n	4.342	4.988	6.268
R^2	0.928	0.967	0.897
Sips			
Qs ($mg \cdot g^{-1}$)	2.423	2.565	1.536
a_s	1.163	0.339	0.141
s	0.794	0.469	0.426
R^2	0.981	0.999	0.916

The estimated parameters derived from each isotherm model are summarized in Table 2-2, with the measured experimental data calculated by a non-linear optimization method. The three-parameter Sips model produced a better fit to the experimental data compared to two-parameter isotherm model, as clearly shown by the value of the correlation coefficient (R^2). The correlation coefficient for the Sips isotherms models varied from 0.916 to 0.990, showing a good fit of the measured data. Conversely, for the Langmuir and Freundlich models, the parameters were obtained with a relatively low correlation coefficient: R^2 = 0.978–0.821 and 0.897–0.967, respectively.

All of the models for the 100 nm MGCN generated very good correlation coefficient values (in the range of 0.928–0.981). Furthermore, the maximum arsenic adsorption capacity derived from both the Langmuir and Sips models were rather consistent. These values (2.3–2.4 mg As(V)/g MGCNs) were higher than those of previously reported for nanoparticle adsorbents such as hematite coated Fe_3O_4 particles (2.1 mg/g),[11] commercial nanomagnetite (0.20 mg/g),[21] and magnetite nanoparticles supported on Fe-hydrotalcite (1.3 mg/g).[22]

The Freundlich isotherm provides an “n” value that is related with adsorption intensity. A high “n” value indicates good adsorption over the entire range of concentrations studied; a low “n” value means that adsorption ability is increased at high concentrations, but is decreased at lower concentrations.[21] The “n” values of the MGNCs were 4.3–6.3 for different size MGNCs, which

were higher than the “n” values of previously reported nanoparticle adsorbents such as commercial nanomagnetite (1.8),[21] magnetic Fe_3O_4@NiO hierarchical structures (2.2),[8] and magnetite-reduced graphene oxide composites (2.9-3.0).[23]

Based on the results of the arsenic removal experiments and the adsorption isotherm model studies, the MGNCs studied in this work seem to have several advantages including: (i) quick, simple, and straight forward preparation, which can be easily scaled-up for mass production; (ii) neither pH nor temperature dependence that is usually needed during the adsorption process (yet they maintain high adsorption capacity which is beneficial for efficient field applications); and (iii) a simple magnetic separation and recovery system that takes advantage of the strong magnetic property of MGNCs.

Arsenic removal from artificial arsenic-contaminated groundwater. In In order to emphasize the applicability of our new MGNC adsorbent to remove arsenate from the natural system, As(V)-contaminated groundwater was artificially prepared from distilled water spiked with arsenate and other commonly found cations and anions, as previously described in the literatures (Table 2-3),[24,25] and the remediation process was tested. One liter of artificial contaminated groundwater spiked with arsenate (0.6 mg/ L) along with the various cations and anions was treated with 1.0 g of 100 nm MGNCs in the Erlenmeyer flask, as shown in Graphical Abstract. The treated water was then separated from the MGNCs by magnetic decantation and the remaining arsenic

concentration in the purified water was determined by ICP-AES. The remaining arsenic concentration was lower than 10 μg/L, implying that our MGNCs successfully adsorbed the arsenate from the artificial arsenic-contaminated groundwater to achieve the WHO prescribed safety limit of arsenic concentration in drinking water.

Table 2-3. Composition of artificial arsenic-contaminated groundwater

Ion	Na^{+}	Mg^{2+}	Ca^{2+}	HCO_3^{-}	SiO_3^{2-}	PO_4^{3-}	SO_4^{2-}	Cl^{-}
mg/L	145	8	51	363	12.5	1.93	32	90.3

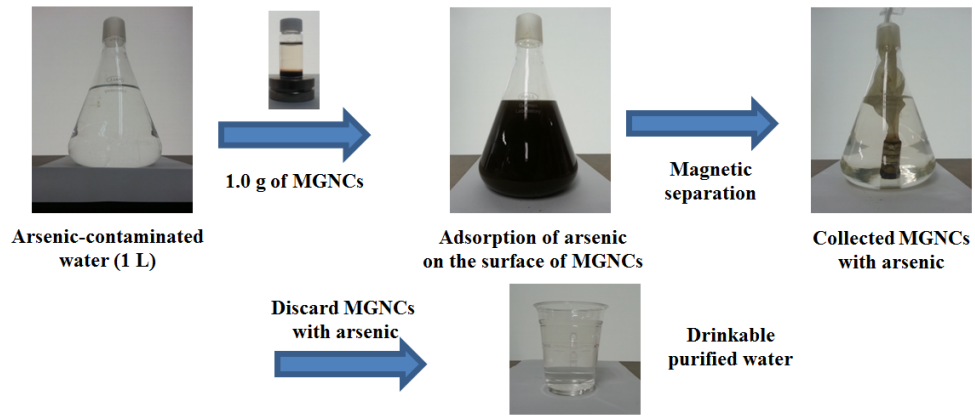

Figure 2-7. Graphical Abstract.

2.4. Conclusion

Ferromagnetic multi-granule nanoclusters which can be synthesized on a large scales with reasonably high magnetic saturation values of 74-85 emu/g and good dispersion properties in water despite their relatively large size in the range of 100-400 nm, were successively employed as new adsorbents for removing arsenic contaminant from water. Adsorption equilibrium data were fitted to the Langmuir, Freundlich, and Sips isotherm models and the various resulting parameters were evaluated. The findings of this work are significant because they show that 1 L of artificial arsenic contaminated groundwater (0.6 mg/L of arsenate) could be effectively remediated with 1.0 g of 100 nm MGNCs, which complied with the WHO permissible arsenic limit of 10 μg/L in drinking water. From these results, we expect that magnetic MGNCs can effectively remove arsenic from contaminated groundwater at a considerably low cost that will make it suitable for application in household- or small-scale water treatment system, after a more precise kinetic investigation of the adsorption processes is conducted.

2.5. References

(1) Mohan, D.; Pittman Jr, C. U. *J. Hazard. Mater.* **2007**, *142*, 1.

(2) Nguyen, T. V.; Vigneswaran, S.; Ngo, H. H.; Kandasamy, J. *J. Hazard. Mater.* **2010**, *182*, 723.

(3) Brammer, H.; Ravenscroft, P. *Environment International* **2009**, *35*, 647.

(4) *Guidelines for Drinking-water Quality*; 3rd ed.; World Health Organization: Geneva, **2008**.

(5) Rubel, F., Jr. *Removal of Arsenic from Drinking Water by Adsorptive Media*; USEPA, **2003.**

(6) Ronkart, S. N.; Laurent, V.; Carbonnelle, P.; Mabon, N.; Copin, A.; Barthélemy, J.-P. *Chemosphere* **2007**, *66*, 738.

(7) Malik, A. H.; Khan, Z. M.; Mahmood, Q.; Nasreen, S.; Bhatti, Z. A. *J. Hazard. Mater.* **2009**, *168*, 1.

(8) Zhang, S.; Li, J.; Wen, T.; Xu, J.; Wang, X. *RSC Advances* **2013**, *3*, 2754.

(9) Wu, Z.; Li, W.; Webley, P. A.; Zhao, D. *Adv. Mater.* **2012**, *24*, 485.

(10) Steven, L.; Nathan, B.; Jisoo, K.; Parsons, J. G. *Microchem. J.* **2012**, *101*.

(11) Simeonidis, K.; Gkinis, T.; Tresintsi, S.; Martinez-Boubeta, C.; Vourlias, G.; Tsiaoussis, I.; Stavropoulos, G.; Mitrakas, M.; Angelakeris, M. *Chem. Eng. J.* **2011**, *168*, 1008.

(12) Manceau, A. *Geochim. Cosmochim. Acta* **1995**, *59*, 3647.

(13) Farrell, J.; Chaudhary, B. K. *Environmental Science & Technology* **2013**, *47*, 8342.

(14) Waychunas, G. A.; Rea, B. A.; Fuller, C. C.; Davis, J. A. *Geochim. Cosmochim. Acta* **1993**, *57*, 2251.

(15) Fendorf, S.; Eick, M. J.; Grossl, P.; Sparks, D. L. *Environmental Science & Technology* **1997**, *31*, 315.

(16) Gallegos-Garcia, M.; Ramírez-Muñiz, K.; Song, S. *Miner. Process. Extr. Metall. Rev.* **2011**, *33*, 301.

(17) Cha, J.; Lee, J. S.; Yoon, S. J.; Kim, Y. K.; Lee, J.-K. *RSC Advances* **2013**, *3*, 3631.

(18) Kundu, S.; Gupta, A. K. *Chem. Eng. J.* **2006**, *122*, 93.

(19) Ho, Y. S.; Porter, J. F.; McKay, G. *Water, Air, Soil Pollut.* **2002**, *141*, 1.

(20) Maliyekkal, S. M.; Philip, L.; Pradeep, T. *Chem. Eng. J.* **2009**, *153*, 101.

(21) Türk, T.; Alp, İ.; Deveci, H. *Journal of Environmental Engineering*

2010, *136*, 399.

(22) Türk, T.; Alp, İ. *Journal of Industrial and Engineering Chemistry*.

(23) Chandra, V.; Park, J.; Chun, Y.; Lee, J. W.; Hwang, I.-C.; Kim, K. S. *ACS Nano* **2010**, *4*, 3979.

(24) Arifin, E.; Cha, J.; Lee, J. K. *Bull. Korean Chem. Soc.* **2013**, *34*, 2358.

(25) Hug, S. J.; Leupin, O. X.; Berg, M. *Environmental Science & Technology* **2008**, *42*, 6318.

Chapter 3

The Influence of Cobalt Nanoparticle Dispersion on the Fischer-Tropsch Synthesis Activity

3.1. Introduction

GTL Overview: Gas-to-liquid conversion (GTL) refers to the process of converting natural gas to synthetic oil. This synthetic oil is then used as fuel as a product based on hydrocarbons.[1] LNG, PNG, and CNG are classified according to their respective transportation technologies, but GTL products in a liquid state at room temperature are long-chain hydrocarbon products identified by the transformation technology of chemical conversion.[2]

Coal, natural gas, and biomass[3] are used as raw materials in the FT process, while the meaning of GTL refers to the conversion of natural gas to pure synthetic oil while removing impurities such as sulfur, aromatic compounds, and metal substances.[4] By refining the synthetic oil, it becomes possible to produce diesel, naphtha, wax, and other liquid compounds based on oil or other special products. This transformation technology is based on Fischer-Tropsch synthesis (henceforth the FT process), which was developed 100 years ago.[5] Technology pertaining to the pre-treatment of gas, a reforming and upgrading process, has reached a mature stage, but the FT process is in the stage of commercialization. New technology is continuously being developed, and currently available technology is applied to the conversion process to enhance the efficiency of the process.[6,7] In addition, mini-GTL technology for application to small-scale gas fields is being developed. The factors influencing competitiveness include the investment cost, operation cost, materials cost,

plant dimensions and technology-enhancing usability of the products.[8] In comparison with the history of the coal-to-liquids (CTL) process, GTL is new technology, and globally commercialized facilities are in fact very rare at this point.

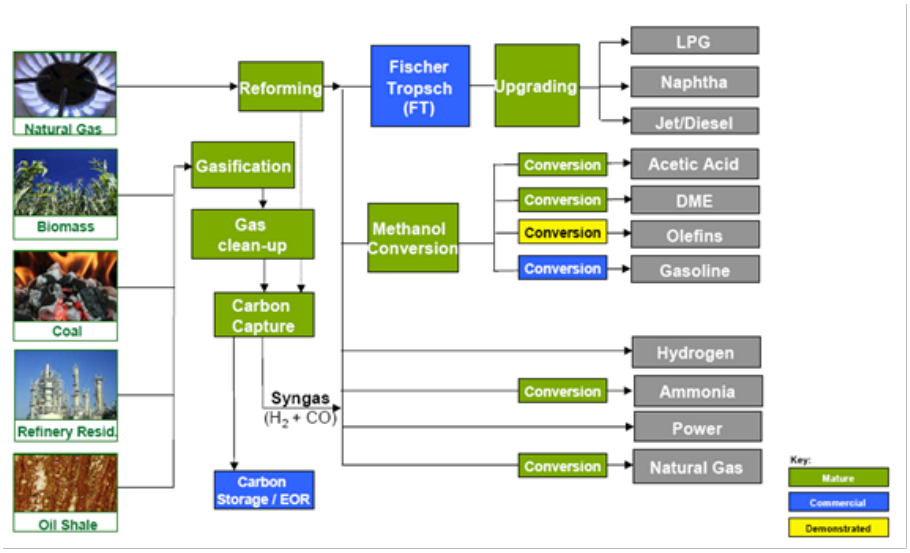

Figure 3-1. Transformation Technology of GTL (source: David Robertson, GTLtec, 18th-19th February **2008**)

Table 3-1. GTL Project Status

Project	Country	Scale	Start-up
Shell Bintulu GTL	Malaysia	14,700	1993
PetroSA Mossgas GTL	South Africa	36,000	1993
Sasol/QP ORYX GTL	Qatar	34,000	2007
Shell Pearl GTL	Qatar	140,000	2011
Chevron Escravos GTL	Nigeria	34,000	2013
Total		258,700	

Figure 3-2. XTL Opportunities across the globe.

(source: http://www.cwcxtl.com)

Through recently a plant in Nigeria was completed, the total GTL production capacity is only 260,000 barrels per day.[9] In contrast, the daily amount of oil consumed worldwide is 87 million barrels. Thus, GTL production is not subject to restrictions set by consumption amounts.

GTL has some advantages in the actual market environment, where the price of oil is high while the gas price remains low. The Figure 3-3 indicates that the development and production of rich shale gas leads to an excessive supply of gas, causing the gas price to fall. Also, the constant demand for oil from China and India tends to increase oil price. The gap between the oil price and the gas price is predicted to increase. One barrel of crude oil generates the equivalent of 5.8 million BTU. In fact, the gas price is less than US $4 per million BTU. When converting gas to oil, a premium of US $13 per million BTU is realized.

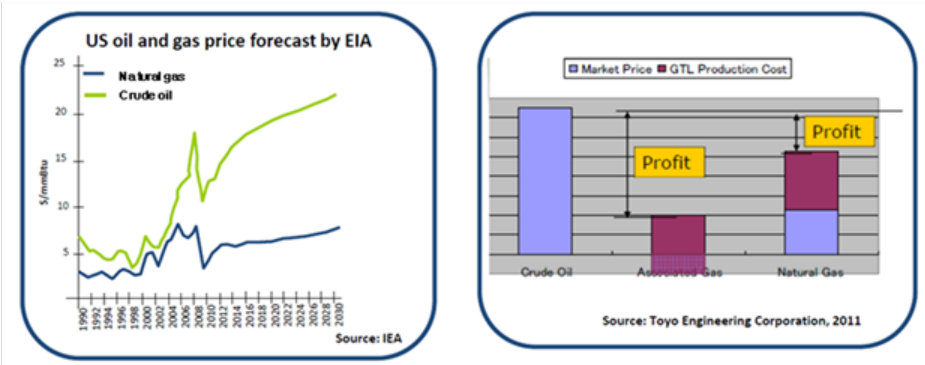

Figure 3-3. US Oil and Gas Price Forecast by EIA and GTL Economy (from Ref. [16] Fonseca, A.; Bidart, A.; Passarelli, F.; Nunes, G.; Oliveira, R. In *World Gas Conference* **2012**)

Mini GTL

For the realization of successful mini-GTL technology, it is necessary to develop compact and high-efficient GTL processes and modularization techniques to ensure competitiveness, even at a small scale.[10-12] Such processes and techniques will be efficient technology when applied to small and medium gas fields as well as oilfield and landfill gas production sites on land and at sea.

GTL technology for developing small and medium gas fields and associated gas sources requires the following conditions: (1) reduction of the plant construction cost for economic feasibility on a small scale for hundreds to thousands of BPD; (2) compactness and mobility for installations in places without infrastructure, such as frozen zones in Siberia; (3) easy installation in limited spaces for offshore applications; and (4) compactness and modularization of compressors and related equipment for a simple process with high efficiency.

Further study will be done for small and medium gas fields, to which mini GTL technology is expected to be applicable. From a long-term point of view, the development of GTL-FPSO linked to shipbuilding technology will be applied to small and medium-scale offshore gas fields as well as the strategy of launching a high-value-added shipbuilding market.

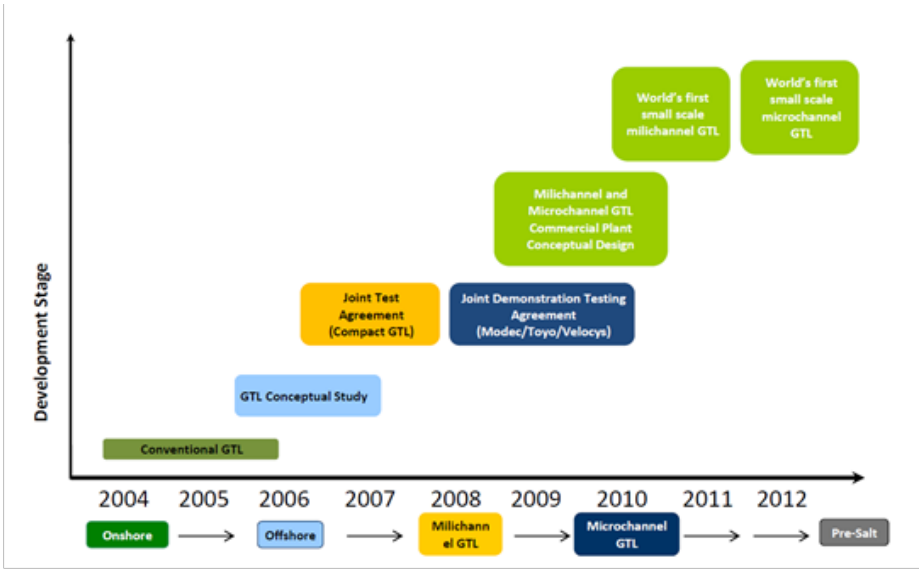

Figure 3-4. PETROBRAS Roadmap toward a Modular GTL Plant (from Ref. [16] Fonseca, A.; Bidart, A.; Passarelli, F.; Nunes, G.; Oliveira, R. In *World Gas Conference* **2012**)

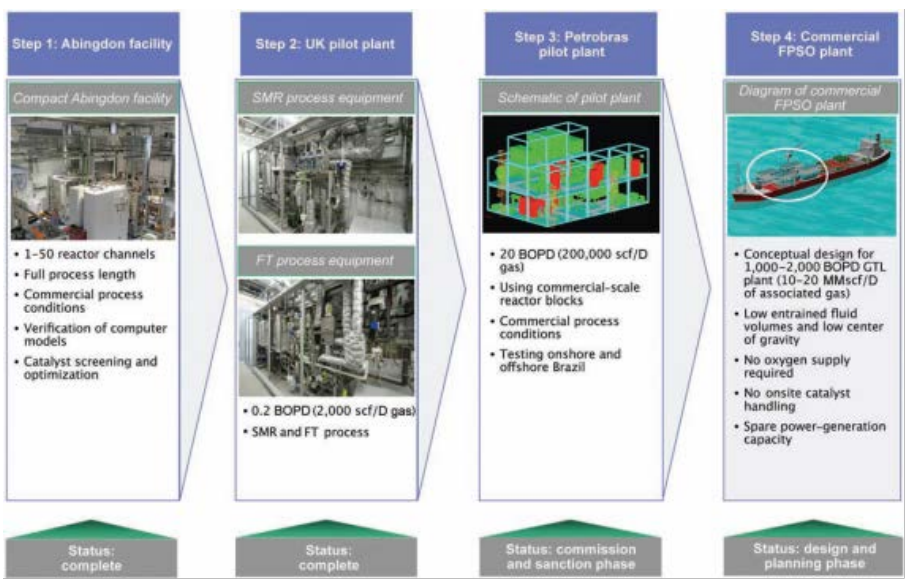

Figure 3-5. COMPACT GTL Roadmap toward a Modular GTL Plant (from Ref.

[13] Hopper, C. *Journal of Petroleum Technology* **2009**, 26.)

The micro-reactor (synthetic gas + F-T synthesis) was developed by CompactGTL, a leading manufacturer of compact GTL technology, and its pilot operation was completed with the application of a 20 BPSD plant with Petrobras in 2011[13]. Moreover, by adopting micro-channel technology, Velocys is developing a mini GTL plant, reporting that a pilot plant capable of producing 2.5 gallons per day has been developed.[14,15] They constructed a 6-BPD plant in Brazil with cooperation from Petrobras, MODEC, and Toyo Engineering, which started its pilot operation in 2012. Given that micro-reaction technology had the advantages of small volumes, high heat transmission and large reactive surfaces and control of the exact reaction time, this technology will enhance the integration of chemical processes, the degree of response selectivity, and the stability.[16]

Fischer-Tropsch synthesis (FTS) reaction

The Fischer-Tropsch synthesis (FTS) reaction is a reaction used for producing hydrocarbon mixtures from a synthesis gas (syngas) containing carbon monoxide and hydrogen produced by the reforming natural gas, the gasification of coal, or from biomass. It is schematically described by reaction (1).

$$nCO + 2nH_2 \rightarrow (CH_2)n + nH_2O \quad (1)$$

The water-gas shift (WGS) reaction (2), a competing reaction that occurs with the FTS reaction (1), produces carbon dioxide and hydrogen by the reaction between carbon monoxide and the water generated from the reaction (1).

$$CO + H_2O \rightarrow CO_2 + H_2 \qquad (2)$$

Consequently, the water generated from reaction formula (1) alters the ratio of hydrogen and carbon monoxide during the overall Fischer-Tropsch synthesis process. In the Fischer-Tropsch process, catalysts having various components and features are used according to the syngas composition as determined by the hydrogen-to-carbon monoxide ratio and the desired products.[17]

There have been many reports of diverse Fischer-Tropsch catalysts prepared with at least one metal selected from Group VIII elements as the major components of the catalysts, with at least one metal as a supplementary promoter or structure-stabilizing agent (U.S. Patent No. 7,067,562).

The carbon number distribution of the Fischer-Tropsch product can change depending on the major active components of the catalyst used. However, generally when a cobalt-based catalyst is used, reaction (1) predominates over water-gas shift reaction (2), and the hydrocarbon (HC) product generally follows the distribution pattern predicted by Anderson-Shulz-Flory (ASF)

theory.

Further, when a cobalt- or ruthenium-based catalyst is used instead of an iron-based catalyst, the reaction may be carried out at a lower temperature. Therefore, a cobalt-based catalyst, which is much less expensive than a ruthenium-based catalyst, is known to be favored for producing paraffin-based hydrocarbons such as liquid or wax, particularly when the feed syngas has a H_2/CO ratio of approximately two. Thus, cobalt-based catalysts have been the subject of extensive studies over several decades. Related to this, several studies have reported increased catalytic activities when certain organic additives are used during the cobalt-based Fischer-Tropsch catalysts synthesis process.[18]

For example, U.S. Patent No. 7,585,808 discloses a catalyst for a Fischer-Tropsch reaction prepared using ruthenium as a catalytic active metal with a triethanolamine treatment. U.S. Patent No. 5,928,983 discloses a cobalt-based Fischer-Tropsch catalyst prepared by adding an oxidative alcohol, oxidative aldehyde or oxidative ketone, especially glyoxal. U.S. Patent No. 5,968,991 discloses a process for activating a catalyst by impregnating a solution containing cobalt, a multifunctional carboxylic acid represented by HOOC-(CRR')n-COOH and rhenium into a refractory inorganic support followed by drying. Several research groups have reported that the dispersion of Co was improved by the use of polyol and ethylene glycol or its homologs.[19-21]

The present study presents a novel cobalt-based catalyst having advanced

catalytic activity and stability together with enhanced selectivity for liquid hydrocarbons and those with high melting points, at the expense of low methane selectivity over conventional cobalt-based Fischer-Tropsch catalysts.

3.2. Experimental Section

Supporting materials

As a silica support, Aerolyst 3041 (SiO_2, excluded type, 0.40 to 0.46 kg/L, 99$^+$%) by Evonik Industries was used. The silica was heated at a rate of 5℃/min to 450℃ and kept at that temperature for 10 hours, after which it was crushed to a mesh size ranging from 100 to 300. BET and other analyses showed that the silica had a specific surface area of approximately 150 m^2/g, a void volume of about 0.80 cm^3/g, and an average pore size of about 20 nm. As an alumina support, gamma-alumina (γ-Al_2O_3, 1/4″x 1/4″white pellets, 15 mg/m^3, 99$^+$%) by Strem was used. The alumina was heated at a rate of 5℃/min to 1,000℃ and kept at that temperature for 5 hours, after which it was crushed to a mesh size ranging from 100 to 300. BET and other analyses showed that the alumina had a specific surface area of about 100 m^2/g, a void volume of approximately 0.30 cm^3 /g, and an average pore size of about 15 nm.

Preparation of Catalysts

Equimolar amounts of $Co(NO_3)_26H_2O$ and one polyether selected from tetraethylene glycol (TEG), tetraethylene glycol dimethylether (TEGDME), poly(ethylene glycol)dimethylether (PEGDME, number-average molecular weight 250 g/mol) and ethanol, 18-crown-6, and 12-crown-4 were added to

distilled water to obtain an impregnation solution having the correct volume to perform incipient wetness impregnation of 8.8 g of the silica support. The resulting mixture was dried at 110℃ for 24 hours, heated to 130℃ at a rate of 1℃/min, kept there at 130℃ for 3 hours, and then heated to 150℃ at a rate of 0.5℃/min and held at that temperature for 3 hours. The dried mixture was then heated to 350℃ at a rate of 0.5 to 1℃/min and kept at 350℃ for 3 hours to obtain a Co/SiO_2 catalyst precursor which on activation contained a cobalt loading of 12 wt%.

Fischer-Tropsch Reaction Test

1g of each catalyst was mixed with 3 g of a diluent (a quartz powder having the same particle size distribution), charged into a high-pressure fixed reactor, and then activated at 723K in a hydrogen gas stream. Then, a mixed gas containing hydrogen and carbon monoxide was introduced, after which the FT reaction was conducted under the following conditions to prepare a hydrogenized product: reaction temperature: 200℃; pressure: 20 bar; $H_2/CO=2$ (containing 4% nitrogen as a GC internal standard); and SV=4000 hr-1 [standard cc syngas/hr•g catalyst (measured at the standard condition of 25℃ and 1 atm). After 15 hours, when the activity of each catalyst was stabilized, an online GC analysis was conducted to examine the activity (mol/g-Co/hr) and selectivity

(%). The results are shown in Table 3-1.

Activity: moles CO converted/g Co hr

Selectivity: moles/100 mole CO converted

Surface Area and FIBSEM Analysis

The specific surface area of the catalysts was characterized using the Brunauer–Emmett–Teller (BET) method by measuring the nitrogen adsorption/desorption surface area (TriStar II 3020, Micromeritics, USA, operated at 77 K).

The three-dimensional microstructure of the catalysts was analyzed using a dual-beam focused ion beam scanning electron microscopy (FIB-SEM) system equipped with an energy dispersive X-ray spectroscopy (EDX) unit (Helios 650, FEI, USA).

3.3. Results and Discussion

Effects of Polyethers on FTS Activity

We examined the effects of diverse polyethers on the FTS activity with a cobalt loading of 12 wt %. In this study, the activity at 15 h on the stream was used as the criteria for the evaluation of the effects of these polyethers. The supported Co catalysts, prepared with polyether and a promoter, were tested in a FT reaction at 20 bar and 200°C at a low CO conversion (< 50 %) rate to screen the polyether and promoter effects. Catalytic activity is expressed as the cobalt time yield (i.e., the number of CO moles converted to hydrocarbons per gram of cobalt per hour). The catalysts prepared using EG, DEG and TEG polyethers showed stable CO conversion characteristics during the FTS reaction condition. The conversions for the catalysts prepared using the polyethers and promoters are shown in Table. 3-2.

A high level of activity was observed for PEGDME and 12-crown-4. The activity levels of Co-PEGDME/SiO_2 and Co-12-crown-4/SiO_2 were stable during the 100 hours of the reaction.

The Co-PEGDME/SiO_2 catalysts showed approximately twice the activity of the Co/SiO_2 catalyst. The Co-TEG/SiO_2 and Co-TEGDME/SiO_2 exhibited slightly higher activity levels than the Co/SiO_2 catalyst, but the organic additive effect was not significant. Co-TEG/SiO_2 and Co-TEGDME/SiO_2 exhibited lower catalytic activity levels than Co-PEGDME/SiO_2. The Co-12-crown-

4/SiO_2 catalysts showed activity that was approximately threefold higher than that of the Co/SiO_2 catalyst. The Co-18-crown-6/SiO_2 catalysts exhibited 0.105 of activity, slightly higher than the activity of the Co/SiO_2 catalyst. Therefore, promoter effect tests were carried out on Co-PEGDME/SiO_2 and Co-12-crown-4/SiO_2.

To study the effects of the promoters, the FTS activity levels of Co-PEGDME/SiO_2 and Co-12-crown-4/SiO_2 with various promoters were investigated with constant amounts of PEGDME and 12-crown-4. In the case of the Co-PEGDME/SiO_2 catalysts, Ni displayed high catalytic activity comparable to the Co/SiO_2 catalyst. It showed an activity level that was more than twice as high as that of the Co/SiO_2 catalyst. However, the Zn promoters exhibited decreased activity, and Al and Cr showed almost no promotional effect. Most of the promoted Co-12-crown-4/SiO_2 catalysts showed a decrease in their activity levels, except for boron, which exhibited an increase. Cu, Cr and Pt showed no promotional effect of the Co-12-crown-4/SiO_2 catalysts, and B-Co-12-crown-4/SiO_2 showed activity that was approximately five times that of the Co/SiO_2 catalyst.

One of the most important requirements for an FTS catalyst is to obtain the maximum conversion of CO while limiting methane selectivity to the lowest level possible. B-Co-12-crown-4/SiO_2 and Ni-Co-PEGDME/SiO_2 exhibited high conversion (47~67%) while directing comparatively little carbon to

methane (<6%). The Co/SiO_2 catalyst also showed a carbon-to-methane transfer, but the conversion rate of CO was lower than 15%, which is not desirable if applying them to the FTS process.

Additional tests were carried out to observe the performance of alumina-supported Co catalysts after an addition of 12-crown-4. Table 3-2 summarizes the activities and product selectivity levels measured after 15 hours of reaction at 20 bar. The alumina showed a moderate polyether additive effect.

As shown in the results of Tables 3-2 and 3-3, the catalyst of Co/SiO_2 not using the polyether compound showed a conversion rate of less than 20%, but the catalyst prepared using polyether showed a much higher conversion rate as high as 70%. Further, the catalyst of the present invention showed lower selectivity to methane and three to five times the activity. Therefore, it is considered that the performances of Co/SiO2 catalysts prepared using polyether are comparable and that they are effective for the synthesis of liquid hydrocarbons from syngas. This finding is of importance to understand the fundamental roles of polyether as an activity enhancer as regards the interaction between Co species and organic additives.

Table 3-2. Test results of the 12 wt% Co/SiO2 catalysts.

Organic	Promoter	X_{CO}	Selectivity				Activ.
			CH_4	CO_2	C_2H_4	C_2H_6	
TEG	-	22.7	9.5	0.2	0.1	0.3	0.106
TEGDME	-	22.6	8.4	0.2	0.1	0.3	0.103
PEGDME	-	31.3	7	0.2	0	0.2	0.144
18-crown-6	-	22.7	12.3	0.2	0	0.6	0.105
12-crown-4	-	38.3	6.6	0.2	0.1	0.3	0.185
PEGDME	Al	31.5	7.2	0	0	0.3	0.156
PEGDME	Zn	23.7	6.4	0.1	0.1	0.2	0.117
PEGDME	Ni	47.2	5.8	0.1	0	0.2	0.233
12-crown-4	Cu	21.8	7.6	0.1	0.1	0.3	0.108
12-crown-4	B	67.2	5.7	0.1	0	0.3	0.331
12-crown-4	Cr	34.2	6.4	0.1	0.1	0.4	0.161
PEGDME	Cr	33.6	6.2	0.07	0.07	0.36	0.156
12-crown-4	Ni	23.8	8.5	0.24	0.07	0.34	0.108
PEGDME	Mn	24	4.9	0.11	0.38	0.3	0.106
12-crown-4	Pt	21	7.1	0.2	0.04	0.28	0.099
PEGDME	Mg	20.3	5.9	0.11	0.21	0.41	0.095
		14.6	6.8	0.3	0.1	0.3	0.065
DEG		19.4	10.1	0.1	0.2	0.9	0.088

Table 3-3. Test results of the 12 wt% Co/Al_2O_3 catalyst.

Organic	Promoter	X_{CO}	Selectivity				Activ.
			CH_4	CO_2	C_2H_4	C_2H_6	
12-crown-4	Zn	46.9	8.9	0.201	0.040	0.361	0.220
12-crown-4	Cr	45.1	7.9	0.163	0.052	0.322	0.212
12-crown-4	B	28.6	7.0	0.096	0.071	0.244	0.134
12-crown-4	Al	27.9	7.4	0.144	0.075	0.275	0.131
12-crown-4	-	27.1	6.6	0.099	0.077	0.218	0.127

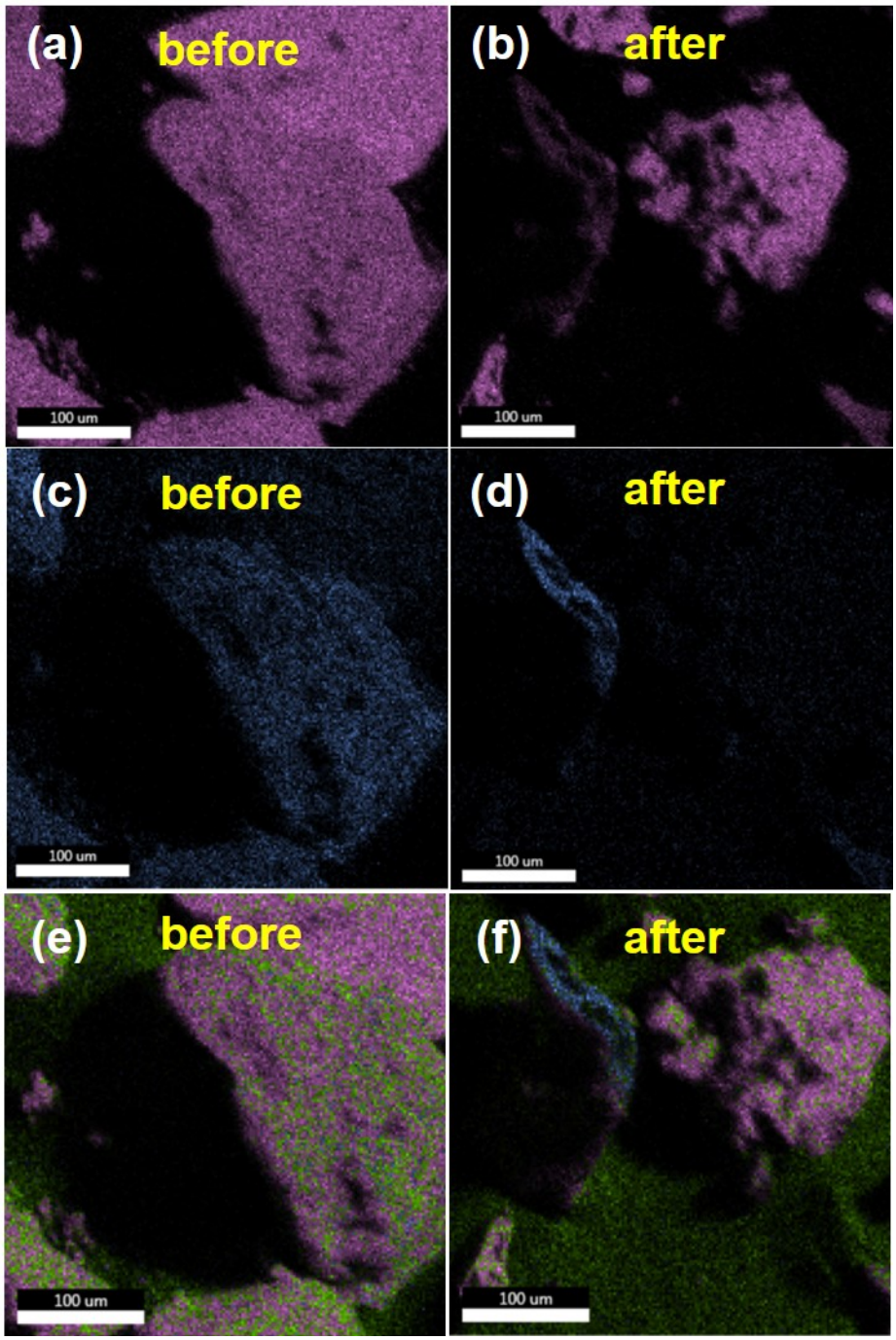

Figure 3-6. Elemental mapping data for Co/SiO_2 with PEGDME before (a, c. e) and after FT-synthesis (b, d, f). (e,f) are merged images. Si is purple, O is green and Co is blue.

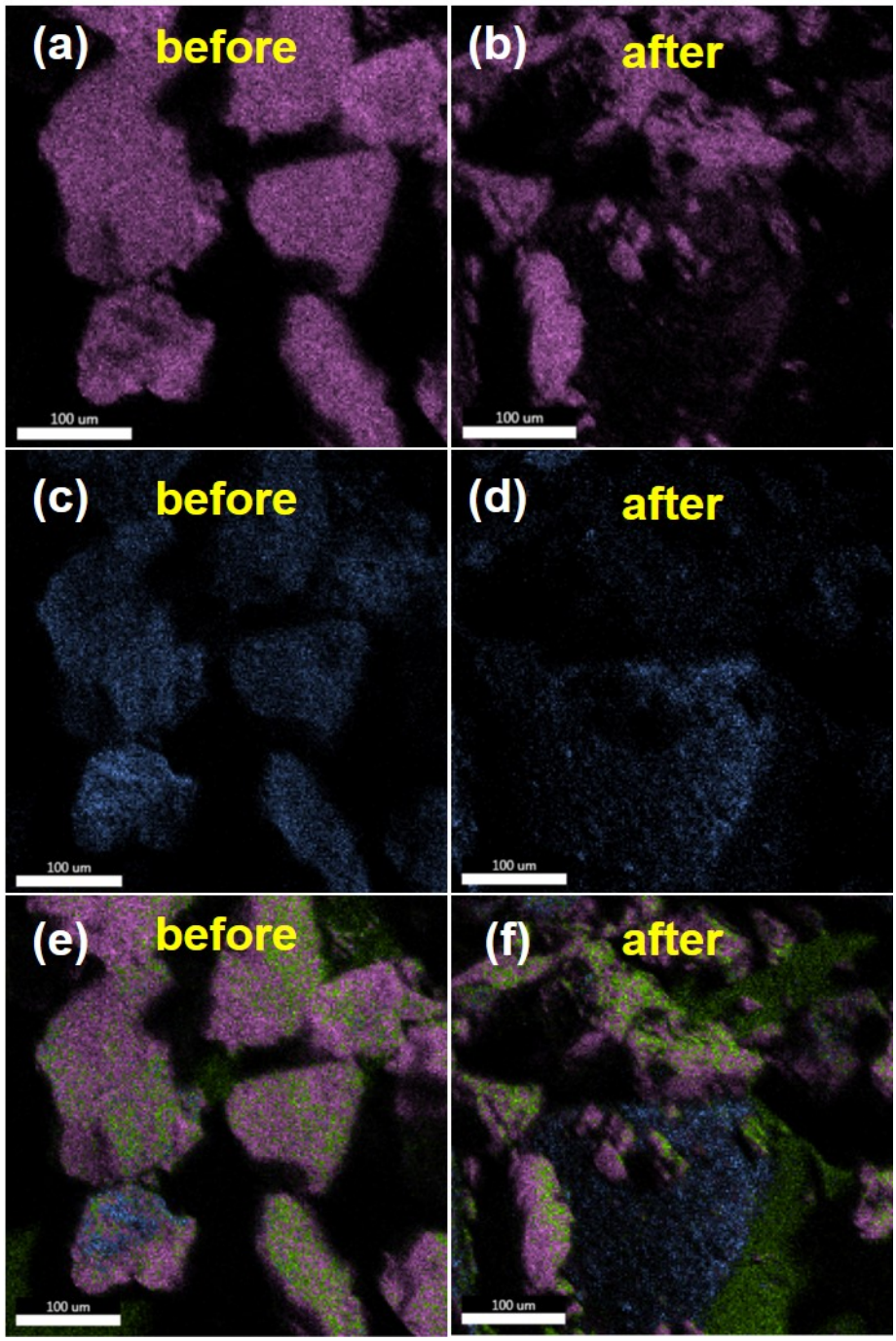

Figure 3-7. Elemental mapping data for Co/SiO_2 with 12-crown-4 before (a, c. e) and after FT-Synthesis (b, d, f). (e,f) are merged images. Si is purple, O is green and Co is blue.

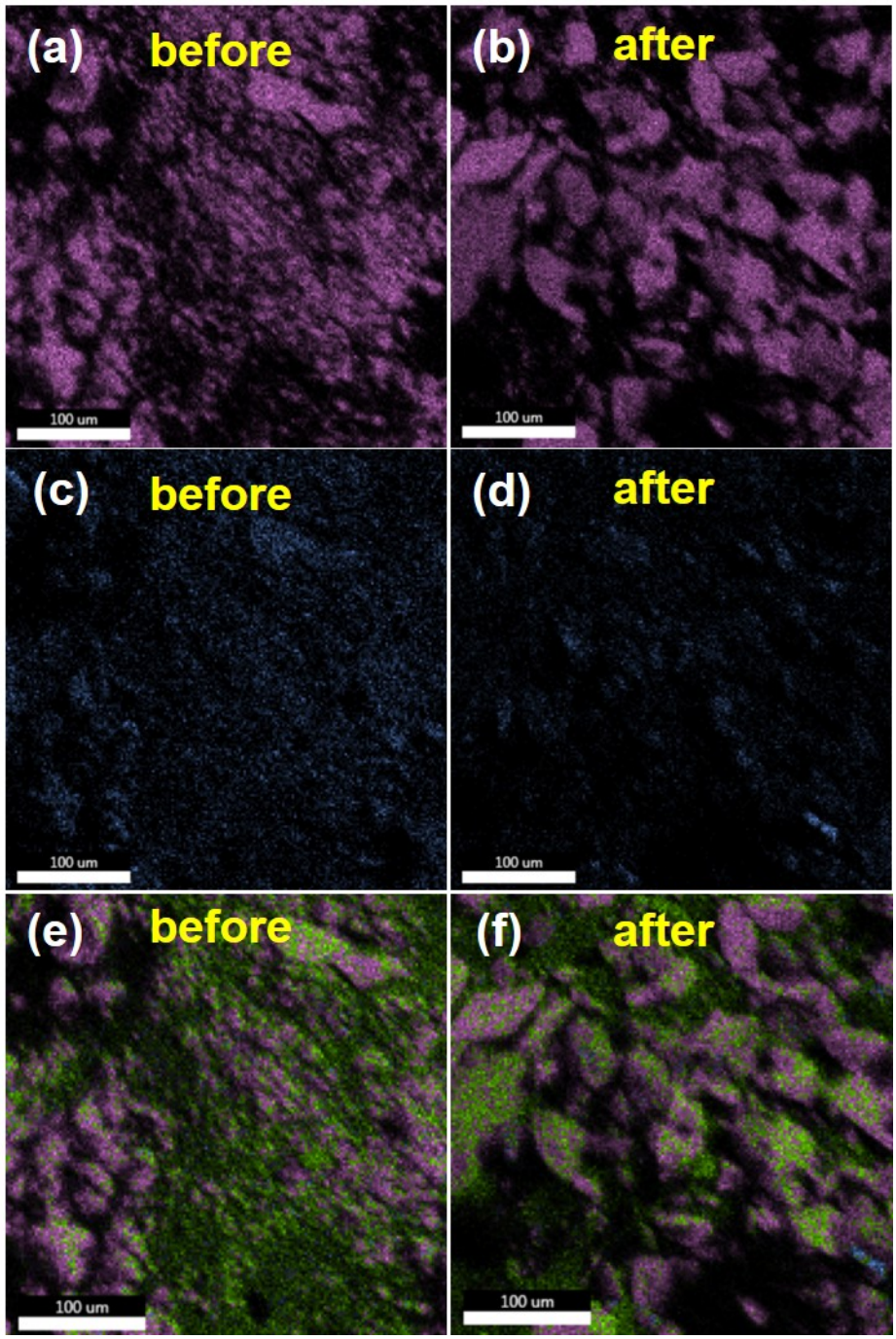

Figure 3-8. Elemental mapping data for Co/SiO_2 before (a, c. e) and after FT-Synthesis (b, d, f). (e,f) are merged images. Si is purple, O is green and Co is blue.

The use of polyether as an organic additive provides a homogeneous distribution of cobalt nanoparticles on a support, in contrast to the extensive clustering that is observed when not using the polyether compound. Co nanoparticle aggregation can lead to low catalytic activity and high methane selectivity, as observed when not using polyether cobalt catalysts. Focused ion beam scanning electron microscopy (FIB-SEM) was used to determine the size of the cobalt oxide particles and their distribution on the support.

Figures 3-6 and 3-7 show a representative FIB-SEM micrograph of the Co-PEGDME/SiO_2 Co-12-crown-4/SiO_2 and catalyst before and after FTS, which exhibits a homogeneous distribution of cobalt oxide particles (blue color). The Co_3O_4 particle size distribution was found to be high. In contrast, the catalyst without the polyether (Co/SiO_2) consisted of large Co_3O_4 particles, which formed aggregates (Fig. 3-8).

FIB-SEM performed on spent catalysts revealed that the cobalt nanoparticles in the supported samples increased in size. The particle size distributions of the fresh and spent Co/SiO_2 catalyst are shown in Fig. 3-8. For Co/SiO_2, low and decreased levels of catalytic activity were observed during the FTS reaction, which suggests that the changes in the catalyst structure took place during the FTS reaction. The spent Co/SiO_2 catalyst consisted of large Co_3O_4 aggregates, which brings about the poor mechanical stability of this catalyst (Fig. 3-8). For the Co-PEGDME/SiO_2 and Co-12-crown-4/SiO_2, the

spent catalyst maintained an average cobalt nanoparticle size and distribution.

Borg et al.[19] noted that the solvent used affects the size and the distribution of Co_3O_4 crystallites. They pointed that while Co_3O_4 appeared in aggregates greater than 100 nm in size when pure water was used as a solvent, these aggregates were absent when ethylene glycol was used as a solvent. When an organic solvent was used for impregnation, aggregates were not present and the Co_3O_4 was more uniformly distributed in the support. The pattern of Co_3O_4 distribution lay between that seen for catalysts based on pure water and pure ethylene glycol. Thus, the degree of aggregation is related to the water concentration of the solvent. Koizumi et al. proposed that chelating agents could be used as an impregnating solution.[20,22] They show a large complex formation constant with Co_2^+. Moreover, it is possible to form a stable chelating agent–Co complex. In relation to organic additives, it is known that alcohols, glycols, and polyol or homologs are ligands for Co_2^+.[20]

Polyether used in this study also forms a strong complex with cobalt. It can be seen that the dispersion of cobalt was increased. It will be able to apply commercial catalyst for FTS, after additional analysis for the relation the particle size and dispersion of cobalt with the reducibility of cobalt and selectivity and productivity for $C5^+$.

3.4. Conclusion

The Fisher-Tropsch synthesis process represents a strong alternative route for the sustainable production of synthetic oil from natural gas. The industrial potential of this process is greatly enhanced by the reported development of active, selective, and mechanically stable catalysts that consist of promoted cobalt nanoparticles dispersed on silica supports. Further suppression of methane production and maximization of the conversion CO with the addition of promoters, polyether and by the optimization of the physical properties (e.g., the Co particle size and/or the distribution of Co nanoparticles on the support) will allow us further to understand and develop the performance levels of these catalysts.

3.5. References

(1) Dry, M. E. *Catal. Today* **2002**, *71*, 227.

(2) Khalilpour, R.; Karimi, I. A. *Energy* **2012**, *40*, 317.

(3) Petrus, L.; Noordermeer, M. A. *Green Chemistry* **2006**, *8*, 861.

(4) Williams, R. H.; Larson, E. D.; Liu, G.; Kreutz, T. G. *Energy Procedia* **2009**, *1*, 4379.

(5) Schulz, H. *Applied Catalysis A: General* **1999**, *186*, 3.

(6) McFarland, E. *Science* **2012**, *338*, 340.

(7) Sousa-Aguiar, E. F.; Noronha, F. B.; Faro, J. A. *Catalysis Science & Technology* **2011**, *1*, 698.

(8) Wood, D. A.; Nwaoha, C.; Towler, B. F. *Journal of Natural Gas Science and Engineering* **2012**, *9*, 196.

(9) Onwukwe Stanley, I. *Journal of Natural Gas Science and Engineering* **2009**, *1*, 190.

(10) Almeida, L. C.; Sanz, O.; D'olhaberriague, J.; Yunes, S.; Montes, M. *Fuel* **2013**, *110*, 171.

(11) Almeida, L. C.; Echave, F. J.; Sanz, O.; Centeno, M. A.; Arzamendi, G.; Gandía, L. M.; Sousa-Aguiar, E. F.; Odriozola, J. A.; Montes, M. *Chem. Eng. J.* **2011**, *167*, 536.

(12) Ha, K.-S.; Kwak, G.; Jun, K.-W.; Hwang, J.; Lee, J. *Chem. Commun.* **2013**, *49*, 5141.

(13) Hopper, C. *Journal of Petroleum Technology* **2009**, 26.

(14) LeViness, S.; Deshmukh, S.; Richard, L.; Robota, H. *Top. Catal.* **2013**, 1.

(15) Atkinson, D. *Biofuels, Bioproducts and Biorefining* **2010**, *4*, 12.

(16) Fonseca, A.; Bidart, A.; Passarelli, F.; Nunes, G.; Oliveira, R. In *World Gas Conference* 2012.

(17) Van Der Laan, G. P.; Beenackers, A. A. C. M. *Catalysis Reviews* **1999**, *41*, 255.

(18) Iglesia, E. *Applied Catalysis A: General* **1997**, *161*, 59.

(19) Borg, Ø.; Dietzel, P. D. C.; Spjelkavik, A. I.; Tveten, E. Z.; Walmsley, J. C.; Diplas, S.; Eri, S.; Holmen, A.; Rytter, E. *J. Catal.* **2008**, *259*, 161.

(20) Koizumi, N.; Suzuki, S.; Niiyama, S.; Shindo, T.; Yamada, M. *Catal. Lett.* **2011**, *141*, 931.

(21) Mauldin, C. H.; Exxon Research and Engineering Company: US, 2001; Vol. US 6,331,575 B1.

(22) Mochizuki, T.; Hara, T.; Koizumi, N.; Yamada, M. *Catal. Lett.* **2007**,

113, 165.

초 록

비소 제거 및 피셔–트롭쉬 반응에서 나노입자의 크기 효과

이 승 호
협동과정 나노과학기술전공
대학원
서울대학교

금속 산화물 나노입자는 고유한 광학, 전기, 자기, 화학 및 기계적 특성으로 인하여, 여러 분야의 기초 연구 및 기술적 응용분야에서 관심과 중요성이 증가하는 분야이다. 또한 금속 산화물 나노입자는 수질에서 발생하는 중요한 환경 공정 및 합성 연료 공정에서의 촉매와 관련성이 커지고 있다. 이 논문에서는 환경과 촉매분야에 응용하기 위한 철과 코발트 산화물 나노입자에 대하여 설명한다.

1 장에서, 자석 산화철 나노입자, 석유 및 가스분야에서 나노 및 코발트를 기반으로한 피셔-트롭쉬 합성 촉매의 설계, 합성 및 활용에 대하여 간략히 요약하였다.

2 장에서, 수질 환경, 특히 인간이 음용하는 지하수로부터 비소를 효과적으로 제거하기 위한 경제성 있는 수단으로써 자성 다중 그래뉼 나노클러스터 (MGNCs)를 연구하였다. 여러 초기 비소 농도에 대

한 비소 흡착 능력 및 효율을 결정하기 위하여 여러 가지 크기의 MGNCs 을 시험하였다. MGNCs는 비소 흡착 특성에 높은 효율을 나타내었고, 세계보건기구가 제시한 안전 허용 기준인 10 μg/L (ppb)를 만족하였다. 0.4 g/L 및 0.6 g/L의 MGNCs로 각각 0.5 mg/L 및 1.0 mg/L 농도의 수중 비산염 (AsO_4^{3-})을 처리하는데 충분하다는 것을 확인하였다. 매개변수를 계산하기 위하여 MGNCs에 대한 흡착 등온 모델을 사용하였다. Langmuir 및 Sips 양쪽 모델에서 유사한 매개변수를 나타냈는데, 이 연구에서의 흡착 공정이 낮은 비소 농도 범위에서도 활성이 있는 것으로 확인되었다. 방해 이온을 포함하고 있는 0.6 mg/L 비산 농도의 인공 비소 오염 지하수 1 L를 가지고 비산 제거 실제 효율을 시험하였다. 이 경우, pH나 온도 조절 없이 1.0 g의 100 nm MGNCs 이면 충분히 WHO가 인정하는 음용수 안전 기준 이하로 비소 농도를 감소시킬 수 있었기 때문에, 실제 현장에서 활용하는데 매우 큰 장점을 가지고 있다.

3 장에서, 피셔-트롭쉬 합성 반응은 천연가스 개질, 석탄 가스화 또는 바이오 매스로부터 생성된 일산화탄소와 수소를 포함하는 가스 혼합물 (합성 가스)로부터 탄화수소 화합물을 생산하는데 활용되는 반응이다. 이 연구에서 기존의 코발트 기반 피셔-트롭쉬 촉매에 비하여 촉매 활성과 안정이 향상됨과 동시에 액체 및 높은 융점의 탄화수소에 대한 선택성은 증가되고 메탄 선택성이 감소된 새로운 코발트 기반 촉매를 제시한다. 우리는 실리카 지지체에 균일하게 분산된

코발트 나노입자 (폴리에테르와 조촉매를 사용하여)를 사용하여 5배 향상된 FTS 활성으로 합성가스에서 $C5^{+}$로 전환시키는 결과를 제시하였다..

주요어 : 비소 제거, 철 산화물, 자석 나노입자, 피셔-트롭쉬 합성, 코발트 산화물, 입자 크기 효과

학 번 : 2004-30162